MAGNETIC TUNNEL JUNCTIONS WITH PERMALLOY LAYERS: A THEORETICAL INSIGHT

Master of Technology

In

Nanoelectronics

Submitted by

Khushabu Gautam

Roll No -77157

Under the Supervision

Dr. Ram Krishna Ghosh

Special Centre for Nanoscience (SCNS)

Jawaharlal Nehru University (JNU)

New Delhi-110067

RECOMMENDATION FORM FOR EVALUATION BY THE EXAMINER/S

CERTIFICATE

This is to certify that the dissertation/thesis **"Magnetic tunnel junctions with permalloy layers: A theoretical insight"** submitted by **Ms. Khushabu Gautam** in partial fulfillment of the requirements for award of degree of **M.Tech** of Jawaharlal Nehru University, New Delhi, has not been previously submitted in part or in full for any other degree of this university or any other university/institution.

We recommend this thesis/dissertation be placed before the examiners for evaluation for the award of the degree of **M.Tech**.

Ram Krishna Ghosh

Signature of Supervisor

Date: 01/10/2021

Signature of Dean/Chairperson

Date: 01/10/2021

Special Centre for Nano Sciences ★ JNU, New Delhi-67 ★ Chairperson

ACKNOWLEDGEMENT

I am highly obliged to express my gratitude and deep regards to my supervisor **Dr. Ram Krishna Ghosh,** for providing me with the opportunity to work under his guidance. I feel extremely blessed to work with him as he always supported and encouraged me throughout the work, even on my bad days. I am also thankful to him for showing confidence in my work and the freedom he gave me during this time. He is a very friendly and sincere teacher having excellent theoretical and practical knowledge.

I would also like to acknowledge all the faculty, Prof. Bijoy K. Kunar, Dr. Balaji Birajdar, Dr. Satyendra Singh, Dr. Pratima Solanki of the SCNS centre. I wish to thank all my lab mates, batch mates and PhD seniors for their kind help.

I heartily acknowledge my brother Neeraj Gautam for always encouraging and guiding me since my childhood. My cordial thanks to my parents, family and friends for their unconditional support throughout my study, without whose help I could not have completed my project.

Khushabu Gautam

ABSTRACT

In the last two decades, there has been an enormous development in the era of magnetic devices by effectively combining magnetics and spintronics into an extraordinary aspect that provides a shape in the age of memory devices. Meanwhile, the discovery of some other materials and phenomena is being continued to achieve the technology impressively, providing an enhanced set for fundamental blocks that could be utilised in designing transistor-like devices for the future scope.

A metal-insulator-metal (MIM) type structure is the most promising candidate confined to memory-based devices in the spintronic related study. This study aims to analyse the magnetic properties of the ferromagnetic materials and their alloys to obtain effective tunnelling magnetoresistance (TMR) in a MIM-type structure known as magnetic tunnel junction (MTJ).

This thesis presents the theoretical analysis of various ferromagnetic materials and their alloys to study their impact on an MTJ device's performance. Due to their high scaling portability and spin-polarized ability, MTJs are considered as an alternative for a charge-based data storing cell. The density of states (DOS) and bandstructures have been calculated in density functional theory (DFT) with the help of Quantum ATK tool using the first principle calculations. An MTJ device contains many interesting characteristics as tunnelling magnetoresistance (TMR), parallel and antiparallel resistances, and spin-transfer torque (STT) components in both in-plane (IP) and out-of-plane (OOP) geometry and these characteristics within the materials have been reported with the help of MTJ Lab tool (NanoHub). TMR is the most important parameters for MTJ. Hence the main concern is to achieve enhanced TMR by simulation work.

Keywords: Tunnelling magnetoresistance (TMR), Antiparallel & parallel resistance, Density functional theory (DFT), Spin transfer torque (STT), Non-equilibrium Green function (NEGF), Gilbert damping coefficient, anisotropy energy.

Table of Contents

List of Figures

List of Tables

List of Abbreviation

Nanometre	nm
Gigabyte	GB
Exabyte	EB
One dimensional	1D
Two dimensional	2D
Three dimensional	3D
Electron-Volt	eV
Complementary metal-oxide semiconductor	CMOS
Ferromagnetic material	FM
Magnetoresistive random access memory	MRAM
Magnetic tunnel junction	MTJ
Tunnelling magnetoresistance	TMR
Spin-transfer torque	STT
Density of states	DOS
Density functional theory	DFT
Local density approximation	LDA
Generalied Gradient approximation	GGA
Non-equilibruim Green function	NEGF

List of Symbols

Curie temperature (T_c)

Resistance of parallel state of MTJ (R_p)

Resistance of antiparallel state of MTJ (R_{ap})

Saturation Magnetization (M_s)

Easy Axis /Uniaxial Anisotropy Field (H_k)

Demagnetization Field (H_d)

Damping Coefficient (α)

Spin Splitting (SS)

Fermi Energy (E_F)

Effective mass of Ferromagnetic (M_{FM})

Effective mass of oxide (M_{ox})

Thickness of Ferromagnetic (t_{FM})

Thickness of oxide (t_{ox})

CHAPTER1

INTRODUCTION

1.1 Motivation

In the current scenario, people rely on technology where they want everything better, faster, and more innovative, also concise as well as in precise form. So today's technology is also concerned about the enhancing performance of devices by reducing the size and increasing their portability. While the continued scaling of transistors faces severe limitations, novel devices incorporating new materials, new transport mechanisms and new state variables are emerging as a strong contender for future logic and memory devices[1].

Hence, we are moving toward dimension reduction and performance enhancement of the devices. As earlier, CMOS technologies were used for memory elements like SRAM, DRAM and flash memory. Undoubtedly, CMOS is a strong candidate for improving power consumption, but the volatility is still a problem with data storage devices and cannot be ignored at present. So these devices are also confined to reduce their size and enhance their volatility. Therefore, we are moving from conventional technology to spintronics in order to enhance the performance of devices. Nowadays, spintronic devices are quite exciting and gaining attention. They are based on electron's spin orientation, which includes the electronic and the spin of conduction electrons to exploit new spin logic devices and advanced data storage memory devices. There is no heat dissipation issue in the pure spin-based currents, and hence it is one of the critical achievements over classical electronics. Thus, to obtain a higher operational efficiency, devices must combine both the charge and spin currents [2].

Today's scaling limits have made a need to acquire electrically accessible memories those are:

- Fast speed
- Low Power
- Embedded ability
- Non-volatility etc.

An MRAM (Magnetic random access memory) is one of the most attractive achievements among spintronics devices in earlier decades. Compared to the usual random access memory (RAM), an MRAM is a more efficient data storage device, which is non-volatile.

The problem with conventional memory is the volatility of information, but in MRAM, data can be retained after removing the power supply which means no loss of data. Hence, researchers would like to introduce volatile and non-volatile memory technologies to replace the most common FLASH and SRAM choices in the appropriate applications, such as magnetic RAM (MRAM) [3].

1.2 Objective

This thesis presents the theoretical studies on Magnetic tunnel junction (MTJ) and exploration of tunnelling magnetoresistance (TMR) for the different types of ferromagnetic materials and their alloys. This study also comprises a glance at Density function theory (DFT) to analyze the structural parameter of every material used in this work. Here, different types of ferromagnetic materials and some of their alloys have been considered to analyze TMR and STT components.

1.3 Thesis Organisation

This thesis is summarized into the following chapters;

- Chapter 2 includes all about the very basic knowledge and theoretical background of the work.
- Chapter 3 comprises the methodology, which has been used for simulation purposes. It includes the basics of NEGF and DFT, and also about the device description.
- Chapter 4 is the result and discussion, including the calculations of bandstructure and DOS of all ferromagnetic materials and permalloys. Also, simulations have been done in this section.
- Chapter 5 is about the conclusion for this complete work.

CHAPTER2

THEORETICAL BACKGROUND

In general, most materials like semiconductors and metals do not show magnetic properties, so there is no meaning of spins and spin-associated moments. Hence, for the study related to the spin-dependent phenomenon, a magnetic material is used. Some of the ferromagnetic materials could be the best-suited candidate as they have the permanent dipole moment to be introduced for the spin and spin-related theory.

A Magnetic tunnel junction (MTJ) device operates on the principle of magnetism; hence it is required to have basic knowledge about the different properties of magnetic and ferromagnetic (FM) materials [4].

2.1Magnetism

Magnetism is a virtue of a material to exhibit magnetic behaviour either in the absence or presence of an applied field. The dipole moment is responsible for magnetism in a material. In the influence of electric field and magnetic field, the motion of an electron is controlled by charge in electronics as well as in magnetism its spin can control it. Generally, any element is said to be a magnet if it carries a permanent dipole moment. Based on their response toward a magnetic field, magnetic materials can be categorized as diamagnetic, paramagnetic, ferrimagnetic, ferromagnetic and antiferromagnetic .

2.2 Spin of Electron

In any material, an electron has a charge as well as a tendency of rotational motion on its axis either in an upward direction or in the downward direction, known as spin. It can be understood as the degree of freedom of an electron. Spin can have a value of either +1/2 or -1/2 at a time. In most materials, equal numbers of the spin are present in opposite directions and they cancel out to each other and no unpaired electrons are present, hence no magnetic behaviour, so these types of materials are referred to as nonmagnetic materials. But, ferromagnetic materials have some uncancelled spin that is responsible for exhibiting magnetic properties. A simple schematic of spin orientation within an electron is represented below (see **Figure 1**).

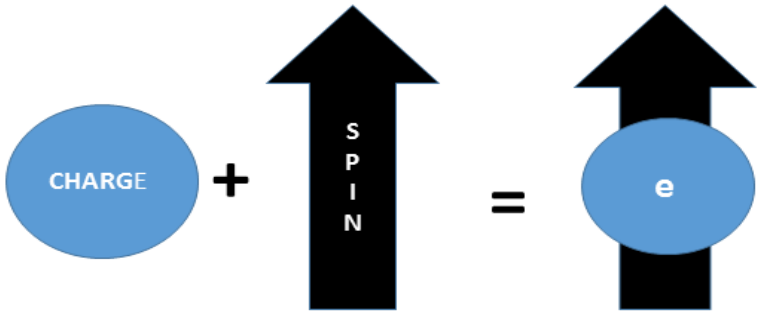

Figure 1. A schematic of the orientation of spin in an electron.

As in the electronics devices where we talk about current generally, we generally understand the motion of charge, whereas the spintronic-based devices are more concentrated on the orientation of spins.

2.3 Ferromagnetism

Ferromagnetism is a material phenomenon that occurs due to the orientation of the net electronic spins in an ordered manner in the presence of an existing field and causes due to a quantum-mechanical exchange interaction. They have a large susceptibility value compared to other magnetic materials, making them easy to get magnetized[5]. A ferromagnet has a certain limit of magnetization that increases in an external magnetic field[6]. Therefore, ferromagnetic materials are characterized by spontaneous magnetization with a non-zero magnetic moment value and defined for a temperature below a specified critical value, and this critical temperature is known as the Curie temperature (Tc). And beyond Tc, because of the random thermal motion, the ordered alignment of spins is destroyed and then the material behaves like paramagnetic material [7].

2.4 Importance of Spintronics

Beyond CMOS innovative work emphasizes stretching out IC technology development into generally advanced approaches in order to determine the best suited for technological enhancement, including the limit of dimensional scaling for CMOS. Consequently, a significant part of the innovation being explored appears unique to the semiconductor innovation of day by day. Nowadays, spintronics is the most exciting field for research with significant applications in various technologies.

In spintronics, the fundamental concept is to manipulate the spin-polarized current in contrast to mainstream electronics, where spins of an electron are not considered. Introducing a spin degree of freedom; provides a new effect, functionality and much capability. In the magnetic multilayers, scattering rates and spin-dependent carrier densities both contribute to the spin-dependent transport mechanism.

At the present range of the system's storage is limited by size. Some are too small as Gigabyte (GB)-based on mobile systems and some require Exabyte (EB) for storage. However, besides their size, the challenge is the same; mostly, computer systems do not consistently run at peak load. Today, information servers require remarkable power measurement in any event when low rates are used.

The requirement of constant refresh is one of the significant issues for the computer system. In an extensive computer system, 33% of its power gets utilized only for power refreshment. And with that power freed up, device users could be operating more powerful and much faster computers.

2.4.1Fundamental elements for Spintronic devices

- Spin generation
- Spin injection
- Spin- transportation from source
- Spin manipulation
- Spin removal

2.4.2 Applications of Spintronic devices

Due to the enhancement of storage and other extraordinary features, MTJs can be used for various purposes. Some of them can be listed as-

- Read / Write heads
- Magnetic memory(MRAM)
- Spin transistors
- Spin diode
- Advanced biomedical devices
- Spin-based sensor and filter
- Quantum computing.

2.4.3 Advantages of Spintronic devices

Based on their performance some advantages can be as-

- Multi-functionality
- Data processing speed increases
- Non-volatility
- Enhanced integration density
- Low power consumption

2.5 Magnetoresistive Random Access Memory (MRAM)

Transistor-based conventional memories, such as DRAM and SRAM, have the problem with volatility that cannot be ignored for future devices. This problem can be overcome by magnetic memory[8] .

A magnetoresistive random access memory (MRAM) is a desirable and promising candidate who can overcome this problem while providing data non-volatility. MRAM consolidates a magnetic device with a microelectronic device to achieve the combined speciality of non-volatility, high-speed operation, limitless "READ" and "WRITE" perseverance, which is not achieved in conventional memories. In MRAM, data can be retained after removing the power supply and hence less power is required than DRAM and SRAM [9]. For the construction of the MRAM structure, several MTJs are joined together either in parallel or in series connection. Here, the two opposite orientations of the magnetization of MTJ are responsible for the recording of binary information and those MTJs are connected to the cross-points of two perpendicular arrays of parallel conducting lines as in **Figure 2(a)** and the cell architecture of an MTJ is shown in **Figure 2(b)**.

MRAM, made of MTJs, is considered to be the next and advanced generation of RAM devices. Some properties are listed as:

- They show very high density
- Fast, reliable reading/writing, non-volatility
- Generally, high power is needed to 'Write' as compared to 'Read'.

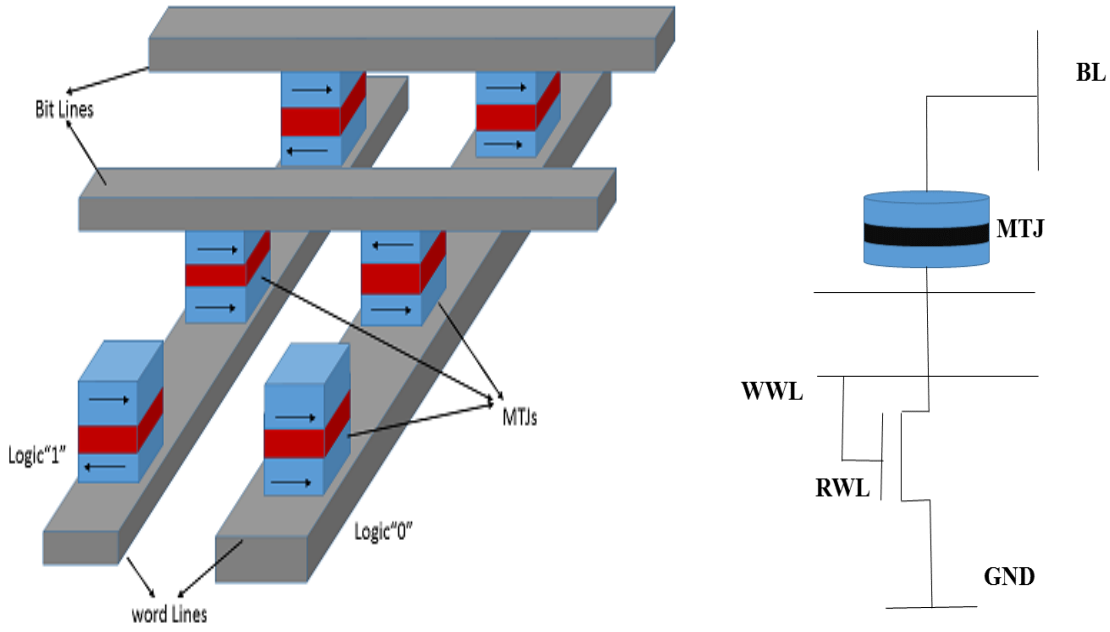

Figure 2. (a) Schematic for the cross-point architecture of an MRAM memory and **(b)**MTJ cell architecture, where WWL and RWL represents 'write word line' and 'read word line' respectively, while BL denotes 'bit line'.

2.6 Magnetic Tunnel Junction (MTJ)

A magnetic tunnel junction (MTJ) is a metal-insulator-metal (MIM) type structure device and one of the most significant spin-dependent devices, where the tunnelling current and tuneable TMR effect can be observed and implemented in other valuable devices. MTJ is a single spin-polarized current controlled device with two input terminals that can realize all logical computation as AND, OR, NAND and NOR logic functions. Some of the application areas of MTJ are sensors, oscillators and RF signal generators etc. An MTJ is a desirable candidate for future magnetic field sensing devices such as random access memories, magnetic field sensors, read-heads, and other applications .

An MTJ is nanostructured two-terminal device consist of three layers. On both sides, the two layers are made of a ferromagnetic material or their alloys. A layer of an insulator (nonmagnetic material) of a few nanometres (nm) is present in the middle of FM layers, usually made of Magnesium Oxide (MgO) or Aluminium Oxide (Al_2O_3). Insulator layer act as a tunnelling barrier[10].

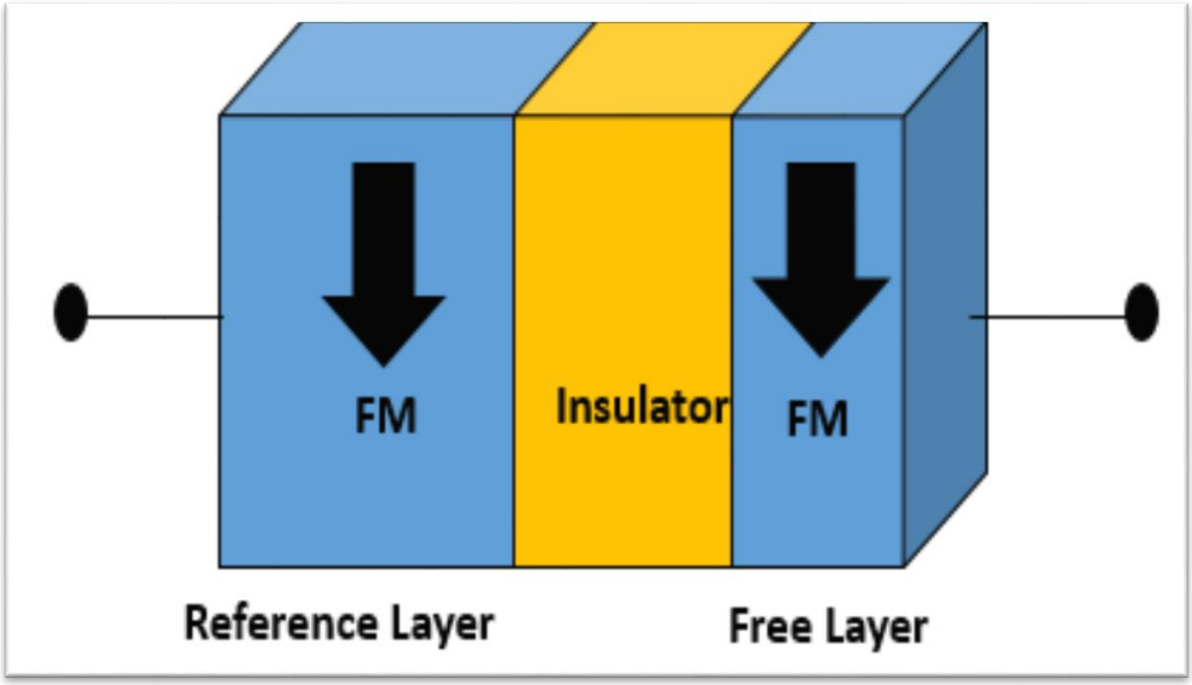

Figure 3. Schematic of the block diagram for an MTJ.

In an MTJ, the first FM layer is kept thicker and fixed, referred to as the reference layer, and the second is called a free layer **(**see **Figure 3)**. An MTJ is analyzed within the magneto-electronics phenomenon where tunnelling current depends upon the relative angle of both FM layers' magnetisation, and it can be varied with the applied magnetic field across them [11].

Multiple input logic functions can be realized by combining many MTJs and transistors in series or parallel configurations. Further, these logic functions can be used for the Arithmetic Logic Unit (ALU) of a computer [12].

2.6.1 Parallel and antiparallel Resistance

Based on the orientation of spins of FM layers, resistance can be defined as parallel and antiparallel resistance. If the alignment of spins is in the same direction, then termed as parallel resistance (R_P), high current (less resistance) and one can understand it as low logic, i.e. "logic 0". And they are termed as antiparallel resistance (R_{AP}) if both FM layers have opposite spins orientation. Here the low current (high resistance) is observed and termed as high logic, i.e. "logic1" **(Figure 4).** This binary logic makes it possible for MTJs to be used as a fundamental element for memory storage [13].

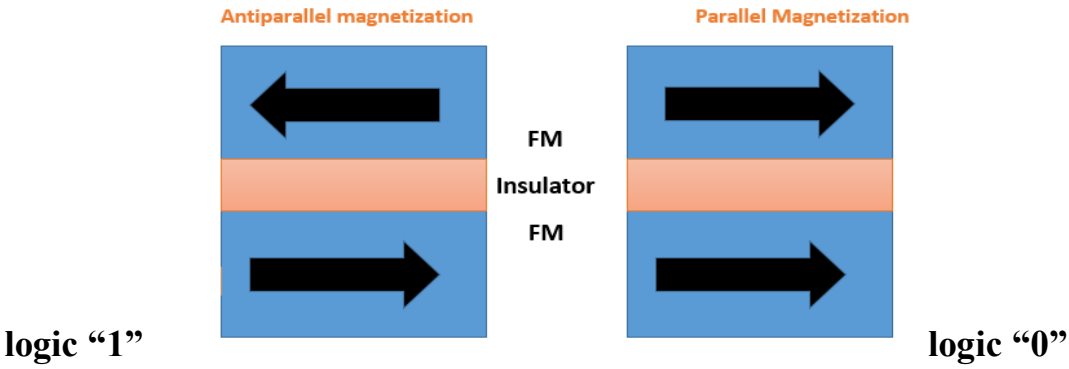

Figure 4. A simplified schematic for high resistance (antiparallel alignment) and the low resistance (parallel alignment) state.

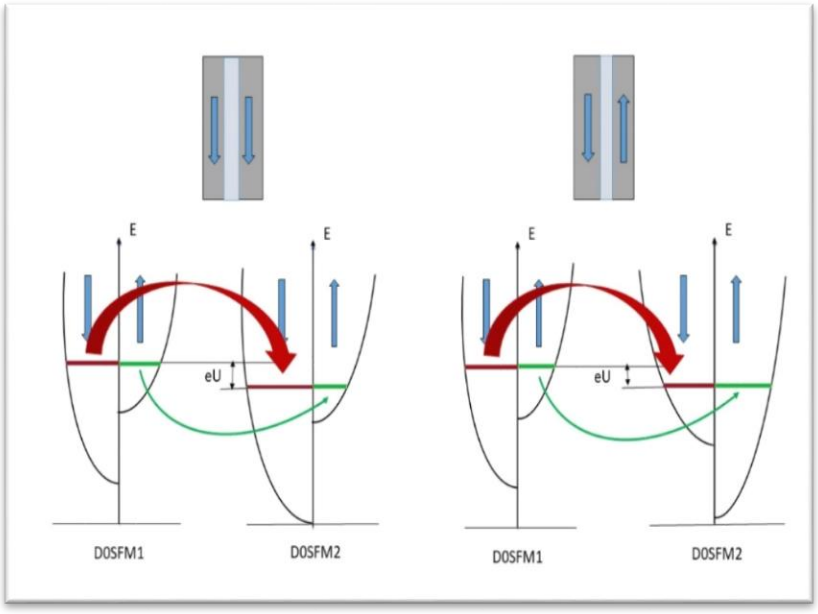

Figure 5 A schematic for alignment of spins- orientation and corresponding DOS in parallel and antiparallel states.

In **Figure 5**, it has shown that how the alignment takes place from the DOS of one ferromagnetic material (FM) to another, and one can observe the differences in both resistance states. In the first condition, spin can easily impose from one to another FM and hence less resistance is required, and it is more difficult to impose in the second condition so high resistance.

2.6.2 Tunnelling Magnetoresistance (TMR)

Magnetoresistance effect is the tendency of a particular material to vary the electrical resistance according to the applied magnetic field. There were two types of magnetoresistance effects

before the discovery of TMR; Anisotropic Magnetoresistance (AMR) and Giant Magnetoresistance (GMR). The fundamental difference between them is the material used for barrier layers. In MTJ, when the barrier layer has been replaced by an insulating layer within a few nanometres (nm) thicknesses, then the TMR effect has observed. In 1975, the first observation of the TMR effect was reported by M. Jullier [14][15].

Hence, Tunnelling Magnetoresistance (TMR) is one of the most exciting parameters in spintronic devices. It is a quantum mechanical phenomenon and occurs in MTJ. Higher TMR is preferred for better distinction of the resistance difference. TMR enables "READ" operation. TMR ratio can be formulated as – $\mathrm{TMR} = \frac{(\mathrm{Rap}-\mathrm{Rp})}{\mathrm{Rp}}$ (I)

Hence, from equation (I), TMR value can be calculated and it can vary from 0.5 to 5 in present generation MTJs. This type of variation in resistance is the basis for the non-volatile memory build using MTJ. A current sense amplifier can detect the resistances of an MTJ while applying a small voltage across to it. Since the magnets exhibit their magnetization virtue naturally, the memory is non-volatile (compared to DRAM) and need not be refreshed. Overall, these properties combine to make MTJ based memory attractive for ultra-low-power operation .

Also, differential tunnelling magnetoresistance (DTMR) can be analyzed by taking differential resistances of antiparallel and parallel states if required.

2.6.3 Spin-Transfer Torque (STT)

In an MTJ, the spin-polarized current is responsible to modify the magnetic layer's orientation and this phenomenon is known as spin-transfer torque (STT). Due to the majority of spins aligned in either direction (up or down), a spin-polarized current is obtained. When a current passes through the reference layer, the current gets spin-polarized. As this current is directed into the free layer, the angular momentum is transferred to this particular layer by modifying its orientation. If both the layers have the same spin orientation, then a low current is obtained (parallel magnetization), and if in the opposite direction, then a high current is obtained (antiparallel magnetization). Hence, these effects can be used to excite the 'oscillations' or to 'flip' the orientation of magnetic materials and these are observed only at the nanoscale range[3].

As described above, the spin-polarized current through free layer can cause it to "flip" between the antiparallel and parallel states by controlling the magnitude and direction of the applied voltage supply. This enables "WRITE" operation for a memory device. An advantage of the

MTJ based memory is that it only requires applying a larger voltage compared to the "READ" operation, which means that a single compact circuit can be used for both "READ" and "WRITE", making the overall footprint in an integrated circuit smaller and portable. The present generation MTJ devices need higher "WRITE" currents compared to DRAM. The switching speeds are still more than a nanosecond (ns), which enables the memories to operate at GHz frequencies. Success in improving these performance parameters will ensure increasing adoption of MTJ based Magnetic-RAM (MRAM) as a replacement for DRAM based memories [16].

Other features that make MRAM attractive are long-term storage without any external power, radiation-hardening (useful for military and space applications), greater projected reliability compared to the flash memories, and size scalability[17].

Nowadays, spin-transfer torque devices have gained more interest because of their capability to write information without any applied external magnetic fields. An STT technology can build the expected MRAM devices, including the requirements of low current at a reduced cost.

Even re-orientation of magnetization needs an excessive amount of current, which is too high for most commercial applications in present days. Hence, this current density must be reduced, but the reduction in current separately is the basis for present academic research in spintronics[11].

2.7Ferromagnetic Materials

A ferromagnetic material is the most suitable candidate for spin-related study. It has a permanent magnetic dipole moment that refers to more spins availability, and we could do the spin-dependent analysis. These are 3d elements having unpaired electrons, exhibit magnetic property and are referred to as ferromagnetic material. A ferromagnetic material has permanent magnetism without any external applied electric field, leading them into a magnetic material. They have some extraordinary properties than normal materials. Most ferromagnetic materials are metallic. Some common ferromagnetic materials (FMs) are Fe, Co, Ni, and some metallic alloys and rare earth materials, also categorize as a ferromagnet. **Figure 6** shows how the DOS vary from normal material to ferromagnetic material, and that's why an FM is an interesting candidate for the study of spintronics.

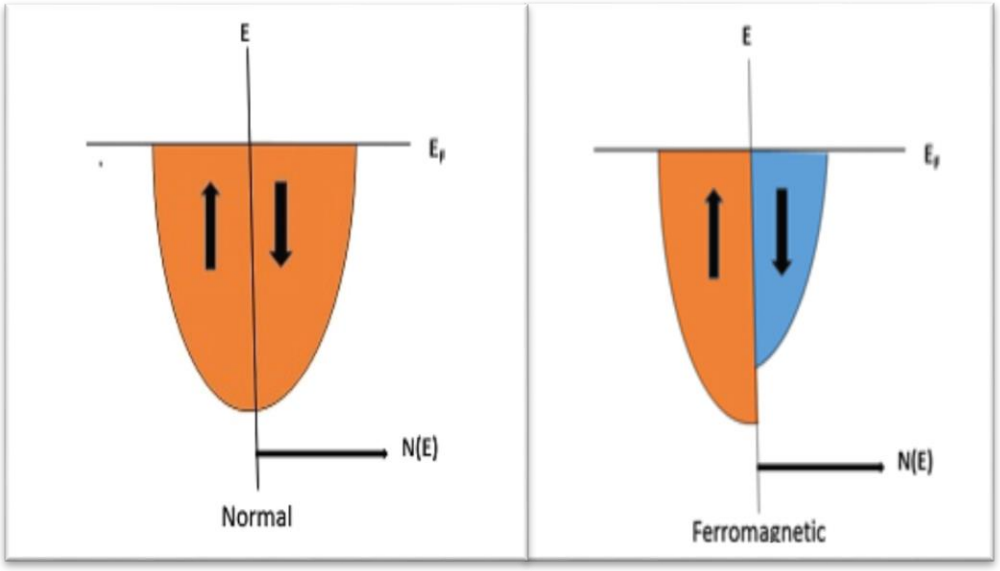

(a) **(b)**

Figure 6(a) Density of state for nonmagnetic material and **(b)** ferromagnetic material**.**

2.7.1 Saturation Magnetization (M_s)

While passing a magnetic field into a ferromagnet (FM), domains got aligned toward the direction of that applied field by its domain boundaries movement. Hence, the magnetization (M) and flux density (B) increased.

Slater-Paulingmode has first successfully described the saturation magnetization (Ms) for the binary 3d transition metal alloys based on a rigid band model. In a simplified manner, while alloying a 3d ferromagnetic material with another material, it causes a shift in the occupation of the magnetic d-states around the Fermi energy, and hence Fermi energy level is changed. And this shifting in an occupation directly results in a changed magnetization which leads to the fundamental triangular shape of the Slater-Paulingcurve by assuming a rigid band model. In the Ni_xFe_{1-x} and Co_xFe_{1-x} alloys, transitions take place from a bcc to an fcc phase, causing a change in the electronic band structure, which leads to the further features of the Slater-Paulingcurve. Also, in Ni_xFe_{1-x} and Co_xFe_{1-x} alloys, magnetic moment with a local minimum is found at the phase.

However, some more magnetic properties as orbital magnetization and magnetic anisotropy exhibit pure quantum mechanical nature and can not be described by semi-classical physics.

2.7.2 Easy Axis or Uniaxial Anisotropy Field (H_k)

Generally, thin films tend to be magnetized in the film's plane, except if there is considerable magneto-crystalline energy which leads to an easy axis perpendicular to the film's plane due to their virtue of thinness. And the magnetization vector remains confined to the film's plane because a large demagnetization field is present perpendicular to the film's plane. There is no predefined direction in film's plane.

If a unidirectional magnetic field is applied in the film's plane while deposition, which results in a single domain configuration with an easy axis parallel to the applied field, also can induce the uniaxial anisotropy field in the film. This anisotropy is termed as magnetization-induced uniaxial anisotropy. For the device fabrication, uniaxial or easy axis anisotropy of thin film is an important attribute and it is characterized by energy dependence in a particular direction[7].

2.7.3 Gilbert Damping Coefficient (α)

In any system, all the material parameters must be well defined to control the spins and alter them according to application. Among those parameters, damping coefficient is a critical parameter of magnetic systems, and it leads the magnetization dynamics of an excited magnetic system towards its equilibrium state. Hence, the operational parameters can be affected by the damping coefficient, such as the critical current or switching speed for STT-driven magnetic switching of a spintronics device. In ferromagnetic materials, damped ferromagnetic precession is an essential mechanism underpinning the magnetization processes.

In a ferromagnetic or nonmagnetic multilayers thin film, damping and precession can play a critical role for the functionality of spintronic device, and as a consequence there has been significant research activity [12]. The dynamics of magnetic relaxation processes in ferromagnetic materials are phenomenologically well described in the Landau-Lifshitz-Gilbert (LLG) equation .

In 1935, Landau and Lifshitz had proposed the first dynamical model for the precessional motion of the magnetization while incorporating quantum-mechanical effects and the effective anisotropy field (H_{eff}) is taken into consideration. Then, the Landau-Lifshitz equation is;

$$\frac{\partial \mathbf{M}}{\partial t} = -\gamma\, \mathbf{M} \times \mathbf{H_{eff}} \qquad \text{(II)}$$

where M denotes magnetic field and γ is the gyromagnetic ratio

The approach followed by Landau and Lifshitz comprises of introducing dissipation in a phenomenological manner[18]. They also introduced an other additional torque term that tries to push the magnetization toward the effective field direction, as represented in **Figure 7**. Then, the Landau-Lifshitz equation becomes;

$$\frac{\partial \mathbf{M}}{\partial t} = -\gamma \mathbf{M} \times \mathbf{H_{eff}} - \frac{\lambda}{Ms} \mathbf{M} \times (\mathbf{M} \times \mathbf{H_{eff}}) \qquad \text{(III)}$$

where λ is a material's characteristic with a positive value, known as the phenomenological constant. It is also important to notice that the additional torque term is choosen such that the magnitude of magnetization is preserved according to the micro-magnetic constraint; $|\mathbf{M}| = \mathbf{M_s}$.

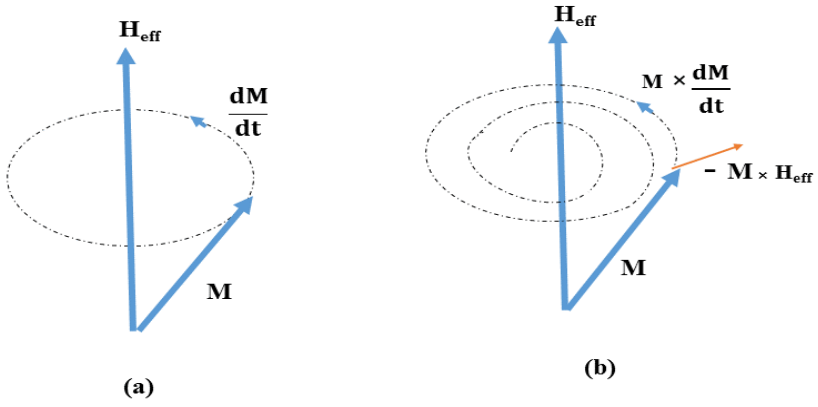

Figure 7. A schematic for the Magnetization precession defined by LLG equation

(a) Before damping **(b)** after damping.

In 1955, Gilbert proposed a different approach, he observed that the conservative equation can be derived with the help of Lagrangian formulation where the components of magnetization vector M is played the role of the generalized coordinates. In this system, the most common approach is to introduce phenomenological dissipation occurs by incorporating a kind of viscous force whose components are directly proportional to the time derivatives of the generalized coordinates. In a more specific manner, he introduces an additional torque term as;

$$\frac{\alpha}{Ms} \mathbf{M} \times \frac{\partial \mathbf{M}}{\partial t}$$

Hence, the precessional equation (III) is modified according to Gilbert's apporoach, and is commonly represented as Landau-Lifshitz-Gilbert (LLG) equation:

$$\frac{\partial \mathbf{M}}{\partial t} = -\gamma\, \mathbf{M} \times \mathbf{H}_{\mathbf{eff}} - \frac{\alpha}{Ms}\mathbf{M} \times \frac{\partial \mathbf{M}}{\partial t} \qquad \text{(IV)}$$

It has been observed that free layer switches the direction at the critical current and it leads the STT-switching in the conventional geometry proportional to the Gilbert damping coefficient (**α**) of the FM. Therefore, the minimization of '**α**' in such systems is crucial for further development in MRAM technology. Gilbert damping parameter with low value can enhance the speed of magnetic solitons [19]. It can also improve the spectral coherence of the oscillators as well as their mutual synchronization properties in spin-torque oscillators. Eventually, the spin currents diffusion is known to be inversely proportional to the '**α**', which is of early-stage significance for devices in spintronics. Heusler alloys are one of the most suitable alternative classes of materials having low value of Gilbert damping, which involves challenging processes for the fabrication. The values of the damping coefficient have been taken for simulation as in **Table1**.

FM	**Damping Coefficient (α)**
Fe	0.002
Co	0.01
Ni	0.063
$Co_{25}Fe_{75}$	0.001
$Co_{50}Fe_{50}$	0.0025
$Co_{75}Fe_{25}$	0.005
$Ni_{25}Fe_{75}$	0.005
$Ni_{50}Fe_{50}$	0.003
$Ni_{75}Fe_{25}$	0.008
$Ni_{25}Co_{75}$	0.011
$Ni_{50}Co_{50}$	0.013
$Ni_{75}Co_{25}$	0.02

Table 1. Values of damping coefficients [20] for the various ferromagnetic materials and their alloys.

2.8 Ferromagnetic Alloys

For the investigation of magnetic phenomena, the 3d transition metals and physical properties of their thin magnetic films are among the most convenient objects [21]. Thin films of metallic alloy, composed of magnetic–magnetic or magnetic–nonmagnetic elements, have regained attention over the past decade because of their magnetic and magnetoresistive attributes. In a magnetic–magnetic system, the conduction electron motion may be affected in a more different manner than that in a magnetic–nonmagnetic system. Some examples for the magnetic–nonmagnetic magnetoresistive systems are FeCu, NiCu, CuCo, while NiFe, CoFe, CoNi alloys system belongs to the magnetic–magnetic systems having high magnetic moments[22]. In this work, various compositions of magnetic-magnetic type alloys are used for the analysis.

2.8.1 Co_xFe_{1-x} Alloys

Co_xFe_{1-x} alloys come under the soft ferromagnetic thin films. They are among the attractive candidates because of their soft magnetic nature, those are high saturation magnetization (M_s), an appropriate anisotropy field (H_k), large uniaxial anisotropy (K_u), low coercivity (H_c), high electrical resistivity (ρ), high permeability (μ), and also good thermal stability as it has a high Curie temperature (T_c) [23] [24]. Co_xFe_{1-x} alloys are useful in several industrial applications as well as in daily life. These alloys have the potential to sustain in microwave absorption applications. They are also widely used in the power generators of aircraft engines and electronic bearings, Read/Write heads, magnetic recording and ultra-largescale integrated devices.

However, the Co_xFe_{1-x} alloys have also been incorporated into micro-electromechanical systems (MEMS), for example; sensors, micro-gears, micro-motors, and micro-actuators. Also, in microwave devices, a fundamental understanding of magneto-static interactions within the thin films is required to know the magnetic inductance, magnetic storage media, and an increased information recording density in these devices; in advanced functional devices, such as spin-valve, magnetic recording media of ultrahigh-density, and wave-absorbing devices; spintronics, magnetic sensors, magnetic random access memory, and so on. Here, **Table 2** indicates all the values for the saturation magnetization (M_s) and uniaxial anisotropy (H_k), which have been used for the different compositions of Co_xFe_{1-x} alloys.

Alloy compositions	M_s(emu/cc)	H_k(G)
Fe	1125	20
$Co_{0.25}Fe_{0.75}$	1375	60
$Co_{0.50}Fe_{0.50}$	1250	88
$Co_{0.75}Fe_{0.25}$	900	180
Co	750	250

Table 2. Values of M_s and H_k [25] for different compositions of Co_xFe_{1-x} alloys.

2.8.2 Ni_xFe_{1-x} Alloys

These types of binary alloys are among the group of materials having high magnetic moment value. Since the early days of magnetic recording, they tend to gain attention continuously. The $Ni_{81}Fe_{19}$ alloy, with a value of 1.0 T saturation flux density, was historically used as the choice of magnetic material for thin-film cores. As it can also be plated into thick films having zero magnetostriction value and soft magnetic properties, it becomes a very desirable candidate in thin-film. This alloy is also corrosion-resistant due to its high Ni-content. It has been used in the first generations of inductive write-magnetoresistive read heads and inductive read-write heads. These alloys had the virtue of soft magnetic properties, higher resistivity, higher moment, and good corrosion properties compared to the Co-based alloys having high-moment; even, they did have highly positive value of magnetostriction. As the areal density of drives increased, the higher-moment materials are needed for more exploration of the higher-iron conent and higher-moment Ni_xFe_{1-x} alloys. These alloys adopt either fcc structure at the Ni-rich side or bcc structure at Fe- rich side.

A list of values for the parameters is shown in the **Table3**, which has been used for further simulation in our work.

Alloy compositions	M_s(emu/cc)	H_k(G)
Fe	1125	20
$Ni_{0.25}Fe_{0.75}$	1050	11
$Ni_{0.50}Fe_{0.50}$	1250	16
$Ni_{0.75}Fe_{0.25}$	800	10
Ni	500	240

Table 3. Values of M_s and H_k [26] for different configurations of Ni_xFe_{1-x} alloys.

2.8.3 Co_xNi_{1-x} alloys

Co-Ni alloys have been widely studied in recent years due to their unique physical and chemical properties. It has been reported that Co-Ni coatings display high adhesion, heat-conductivity, thermal stability, and corrosion resistance, mechanical, chemical, and also superior magnetic properties. Co-Ni coatings could be used as soft magnetic materials and shape memory alloys. It is known that Co-Ni alloys have excellent magnetic properties. Co-Ni alloys have superior permanent magnetic properties than pure metals. Additionally, changing the composition of the magnetic alloys offers a way of modification of their magnetic properties, such as controllable coercivity and improved saturation magnetization. Various methods can be used for the deposition of coatings, such as sputtering, vapour deposition, spin coating and electrodeposition. Nonetheless, except for electrodeposition, these methods are not effective for creating coatings of high-quality and well-controlled magnetic layers. The electrodeposition method has been widely used to fabricate Co-Ni coatings due to the abnormal deposition behaviour of these elements. Electrodeposited Co-Ni alloys have high hardness, excellent wear and corrosion resistance, anti-corrosion, heat-conductive, magnetic, and electro-catalytic properties.

A list of values for the magnetic saturation (M_s) and uniaxial anisotropy (H_k) is shown in the **Table 4**, which has been used for further simulation in our work.

Alloy composition	M_s(emu/cc)	H_k(G)
Co	750	250
$Ni_{0.25}Co_{0.75}$	1250	27
$Ni_{0.50}Co_{0.50}$	900	35
$Ni_{0.75}Co_{0.25}$	700	31
Ni	500	240

Table 4. Values of M_s and H_k for different configurations of Ni_xCo_{1-x} alloys. The references are as follows; M_s [27] and H_k [28].

2.9 Insulator Layer (MgO)

Nowadays, spin-dependent tunnelling between ferromagnetic electrodes separated by an insulating layer is gaining more commercial and scientific interest. The most commonly used insulating layers are aluminium oxide (Al_2O_3) or magnesium oxide (MgO). They work as a barrier between the ferromagnetic layers [29].

Since the discovery of giant tunnel magnetoresistance (TMR) as well as prediction of spin-transfer mechanism and demonstration of spin-dependent coherent tunnelling in MgO-based epitaxial MTJs (in 2001-2004), have an immense contribution to developments in the field of spintronics [30]. In this work, MgO has been used as an insulator layer, and this layer is fixed for all the MTJs of either ferromagnetic material or their permalloys. More further progress in the MgO-based MTJ devices is reviewed by Yuasa [31].

These are some fundamental points to be noticed to understand the enormous TMR obtained in a MgO-based MTJ;

- In the coherent regime, the tunnelling current is established while maintaining the spin and symmetry of the electronic states.
- The current is roughly perpendicular to the (001) interface, while the inclination of trajectories is more attenuated for a thicker MgO -barrier.
- There is no density of state (DOS) for the minority spin along the (001) direction in the reciprocal lattice..
- The MgO –insulator barrier acts as the symmetry filter.

CHAPTER 3

METHODOLOGY

In this section, we will briefly discuss the functions, techniques and tools used in the simulation process.

3.1 Density Functional theory (DFT)

It is a quantum-mechanical modelling approach-based computational method used to study and investigate the electronics structure or nuclear structure (specifically of the ground state) of many body-system into particular molecules and atoms. This theory is useful to determine the properties of a many-electron system [32]. Density functional theory (DFT) is among the most versatile and popular methods available in quantum physics and solid-state physics. DFT has been quite popular for the calculation of electronic structure in solid-state physics since the 1970s. Here, the computational cost is relatively low compared to a conventional method.

DFT gives the minimum or ground energy state proportion of a system, where the density of electron contributes a vital role obtained quantum mechanically after using Schrödinger's Equation[33]. The electron density is denoted by ρ(r) or n(r).

As we know, a wave function (ψ) can contain all the information related to a system, and the wave function can be evaluated by solving the Schrödinger's Equation. By considering a single-electron system with kinetic energy 'K' and having potential energy' U', the Schrödinger's Equation can be given as

$$H\psi = E\psi$$

$$(K+U)\,\psi = E\psi$$

$$-\frac{\hbar^2}{2m}\nabla^2 + U\psi = E\psi$$

Here, E denotes total energy for the system and ∇^2 is Laplacian operator, and in the Cartesian coordinate system, it is defined as;

$$\nabla^2 = \frac{d^2}{dx^2} + \frac{d^2}{dy^2} + \frac{d^2}{dz^2}$$

3.1.1 Fundamentals of Density functional theory (DFT)

- Wave function
- Quantum mechanical operation
- Ground state

3.1.2 Exchange Correlation function (E_{xc})

Generally, this term can be interpreted as having detailed correlation and exchange contributions to the system energy. The exchange-correlation function includes all quantum mechanical terms. The exact form of the exchange-correlation function is not known; hence, to describe this function, the researcher must introduce approximated functions on the basis of the electron density. The two standard approximations are used as [34];

- **LDA:** Local Density Approximation and
- **GGA:** Generalized Gradient Approximation

3.2 Non- Equilibrium Green Function (NEGF)

It is a quantum-transport based mechanism and used for nanoscale device simulation. An efficient self-consistent approach combining the non-equilibrium Green's function (NEGF) formalism with DFT is developed in order to calculate electron transport properties of nanoscale devices [35][36]. NEGF approach is a powerful conceptual tool which provides a practical analysis method to treat small electronic devices quantum mechanically and agonistically[37]. In this approach, bandstructure, electrons correlation effects, layer thickness and applied biasing are taken into account for current calculation. Hence, it can provide a reliable description of the transport mechanism[38].

In both semiconductor and molecular physics, a NEGF is commonly used to calculate current or charge densities at the nanoscale range under bias conditions. Green's function gives the response of a system to a constant perturbation the Schrödinger's Equation [39].

An MTJ lab tool is a NEGF based quantum transport simulation tool used to calculate the critical transports of an MTJ as R_{AP} and R_P, TMR and STT components well. This tool is available online at **nonohub.org** and it has been used to simulate the device parameters (nanoHUB 2018; Datta et al. 2012; Ganguly et al. 2013).

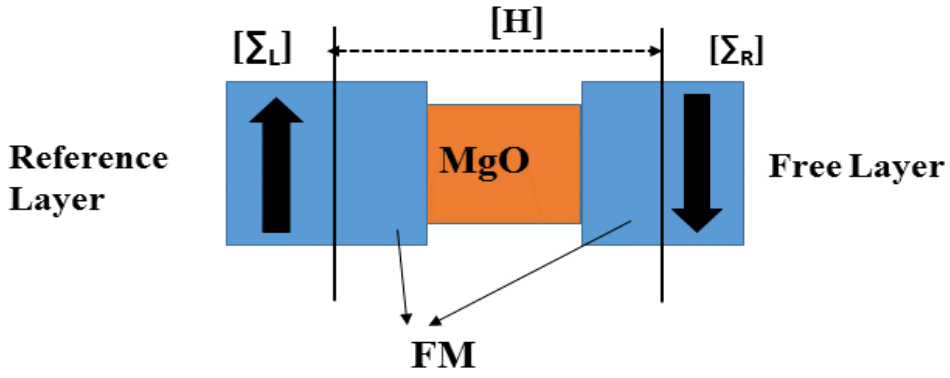

Figure 8. A schematic of the MTJ device in terms of matrices parameter.

This model is realized as a one-dimensional (1D) chain of atoms based upon the effective mass tight- binding. Hamiltonian consists of two FM layers and the oxide layer and the Self-Energy matrices corresponding the large contact regions of both sides. At the interface layer of the tunnel barrier and the free layer of FM, the spin current is calculated. The retarded Green's function (G^R), also known as propagator and the electron correlation is calculated using:

$$G^R = [E - H - \sum_L - \sum_R]^{-1} \quad \text{(V)}$$

$$G^n = G^R (\Gamma_L f_{L+} \Gamma_R f_R) G^A \quad \text{(VI)}$$

where E denotes the energy at which G^R is calculated, H is Hamiltonian and $\sum_L$, $\sum_R$ are self-energy matrices for left and right electrodes of MTJ (see figure 8). G^A is a conjugate transpose of G^R. f_L, f_R represents fermi- function at the E energy and Γ_L, Γ_R are broadening matrices for both electrodes.

In an MTJ, current at any point is calculated using these two equations;

$$I_{ij} = \frac{q}{h} T_r (\Gamma_i G^R \Gamma_j G^A) \quad \text{(VII)}$$

$$I_{ab} = \frac{q}{h} T_r (H_{ab} G^n_{ba} - G^n_{ab} H_{ba}) \quad \text{(VIII)}$$

Equation (VII) provides current between the two terminals i and j and equation (VIII) for the current between any two points a and b. While H_{ab} is an element of a^{th} row and b^{th} column of matrix H. G^n_{ba}, G^n_{ab} and H_{ba} are also defined similarly for respective matrices and T_r denotes transmission parameter.

Using equation (VII), the resistance is calculated and the STT is calculated by equation (VI) at the free layer of the MTJ. These currents are obtained at single energy and single-mode. After that, the total current is calculated using a double integration over all the modes and energies between the Fermi level windows between both the contacts of MTJ (Ganguly et al. 2013)[40].

3.3 Device description

In MTJ devices, various types of parameters are incorporated as magnetic, structural as well as device parameters. Here, constant values for device parameters have been taken based on our device requirement. All these values are kept constant even in ferromagnetic materials and alloys, while structural parameters vary according to the materials used in this device. A schematic for the MTJ device in a simplified manner is shown in **Figure 9**, and to understand the different parameters, the bandstructure of this device is given in **Figure 10**.

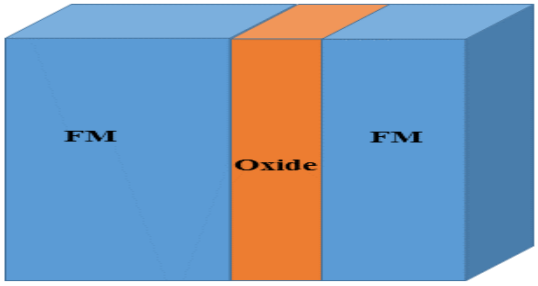

Figure 9. A simple structure for an MTJ device.

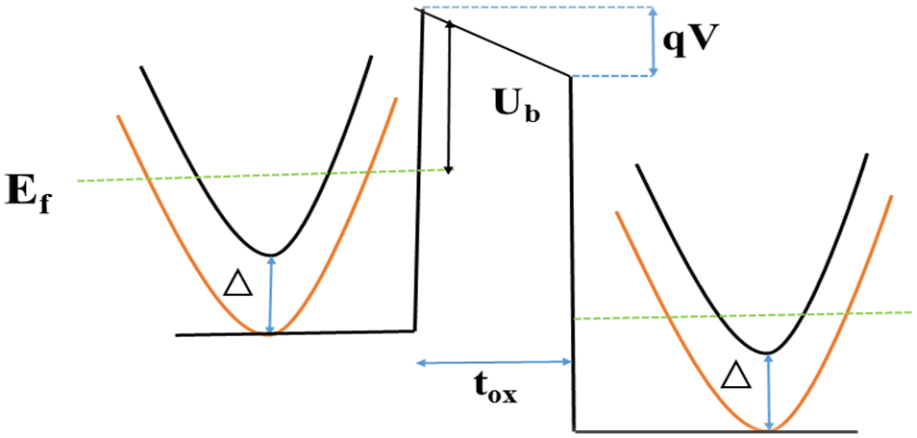

Figure 10. Band diagram for an FM/MgO/FM type MTJ device.

In **Figure 10**, $\mathbf{E_f}$ represents fermi energy level, $\mathbf{U_b}$ is barrier height and $\mathbf{t_{ox}}$ is the thickness for insulator (oxide) layer, Δ represents spin-splitting of ferromagnetic layers and V is biasing voltage between the FM layers. A table for constant device parameters is given in **Table 5**.

Parameters	Value
m^*_{FM}	0.36
t_{FM} (nm)	2
t_{ox} (nm)	1.3
m^*_{ox}	0.36
$A_{FM}(nm^{2)}$	11200
Supply Voltage(V)	-0.4 to 0.4

Table 5. Values of constant parameters for MTJ device [16].

where m^*_{FM} and m^*_{ox} dentotes effective masses for the free layer and insulator layer, respectively, A_{FM} represents the area of the free layer.

Some of the structural parameters as spin-splitting, bandgap and fermi energy has been calculated in the further section.

CHAPTER4

RESULTS & DISCUSSION

4.1 Electronic properties of MgO barrier

The crystal structure of MgO is a cubic cell in rock-salt structure form and this crystal structure can be described as fcc lattice of 'Mg' ions with 'O' ions occupying all the octahedral holes or vice versa. By using DFT, we have analyzed the band structure of the MgO insulator layer. From here, bandgap energy for MgO has been taken and used for further calculation in simulation work.

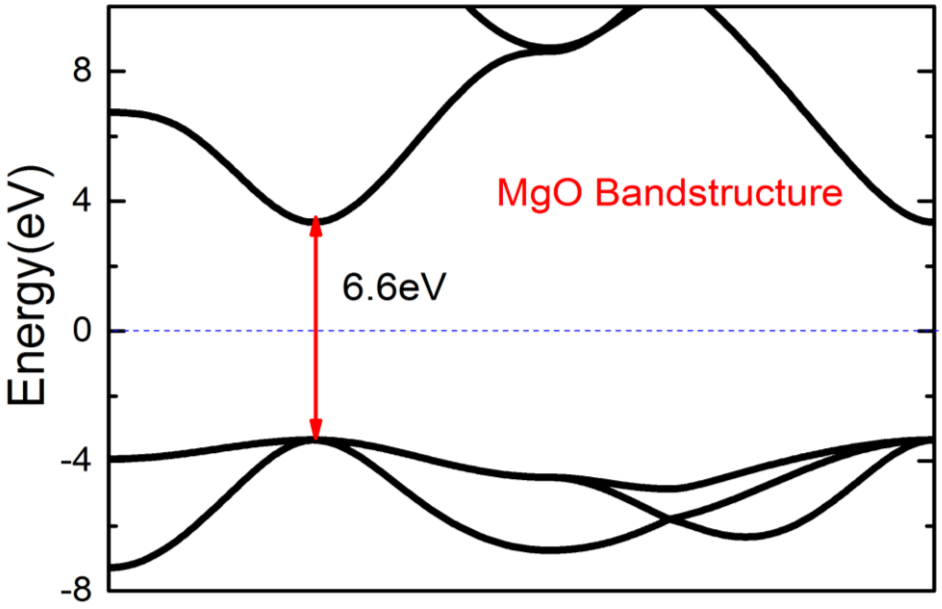

Figure 11. Bandstructure of MgO tunnelling barrier.

In **Figure 11**, a bandgap of 6.6 eV has been obtained for the insulator layer, and half of the bandgap value (i.e. 3.3 eV) is used for further calculation as per the requirement of the simulation tool [4]. After this observation, we have calculated the barrier height (U_b) at the insulator junction for all the ferromagnetic materials and their alloys used as reference layers of MTJ. The barrier height has been calculated as; $\mathbf{U_b = (3.3 - E_f)\ eV}$.

The calculated parameters are given in the **Table 6**. Barrier height (U_b) has the lowest value for Fe among all the FM and $Co_{25}Fe_{75}$ among all the ferromagnetic alloys.

Materials	**Barrier Height(U_b) (eV)**
Fe	0.87
Co	1.12
Ni	2.05
$Co_{25}Fe_{75}$	0.92
$Co_{50}Fe_{50}$	0.96
$Co_{75}Fe_{25}$	1
$Ni_{25}Fe_{75}$	1.25
$Ni_{50}Fe_{50}$	1.15
$Ni_{75}Fe_{25}$	1.07
$Ni_{25}Co_{75}$	1.55
$Ni_{50}Co_{50}$	1.35
$Ni_{75}Co_{25}$	1.15

Table 6. Values for barrier heights for various ferromagnetic materials and their alloys.

Among all other parameters, the barrier height is one of the basic terms for tunnelling to occur. The tunnelling effect can be more effective if barrier height is less so that more chances of carriers to pass through the barrier. Hence, more tunnelling current and other tunnelling-related parameters can be obtained. And TMR effect will reduce as barrier height at the insulator junction increases because there will be fewer spins available to cross the barrier; even others parameters are also responsible for TMR either more or less.

4.2 Density of State (DOS) Calculation

With the help of DFT, the density of states (DOS) of various components as Fe, Co, Ni and their permalloys has been plotted. Based on these structures, spin-splitting has been calculated and has been taken under consideration for the simulation.

4.2.1 DOS calculation for Fe, Co and Ni

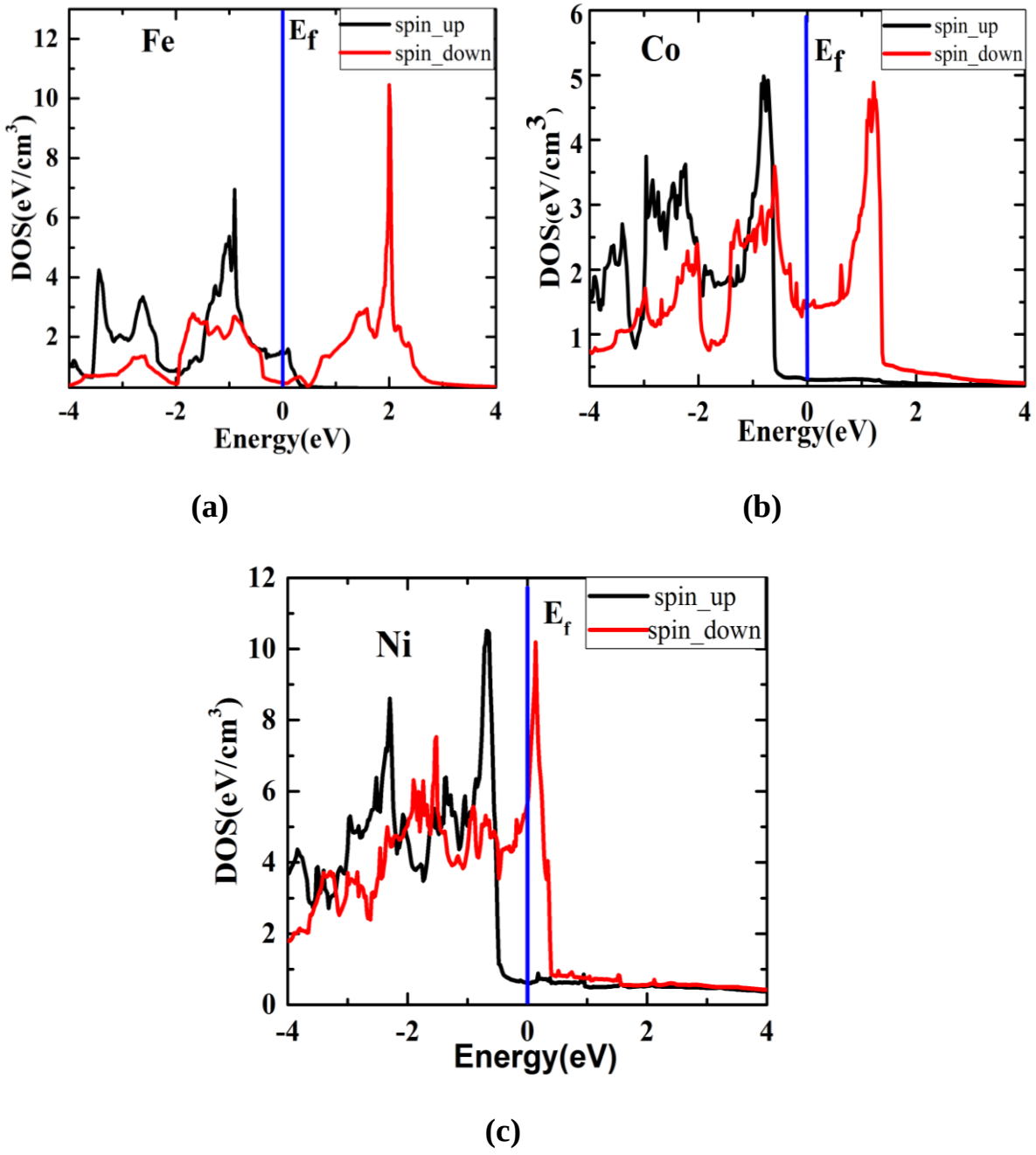

Figure 12. DOS of various ferromagnetic materials **(a)** Fe **(b)** Co and **(c)** Ni

The value of spin-splitting can be calculated by taking the difference between spin-up and spin-down states and from **Figure 12**, it can be observed that the spin-splitting value for the 'Fe' is the largest and lowest for Ni among all the three FMs.

Hence, the calculated values of spin-splitting for all the FMs are listed in **Table 7**. And, these values have been considered for simulation work.

FM	SS(eV)
Fe	2.25
Co	2
Ni	1

Table 7. Values of spin-splitting for various ferromagnetic materials.

4.2.2 For Ferromagnetic alloys

(I) $Co_x Fe_{1-x}$ Alloys

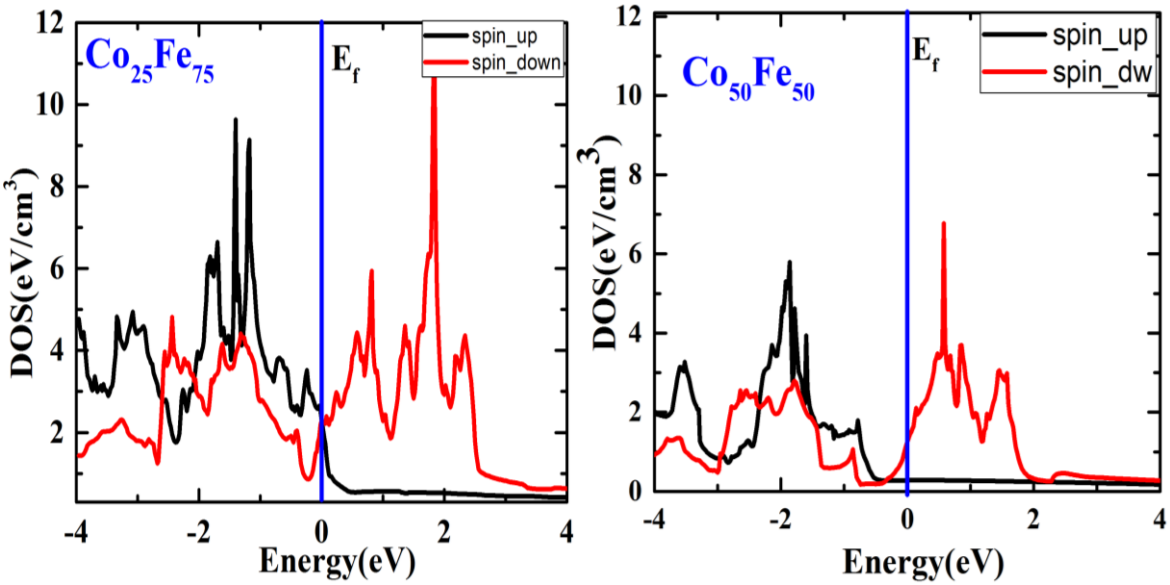

(a) **(b)**

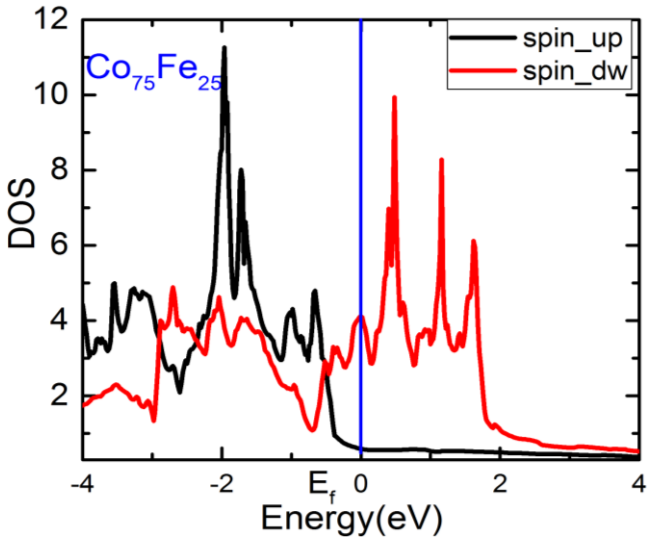

(c)

Figure 13. DOS for the different configurations of Co_xFe_{1-x}.

In **Figure13**, (a),(b) and (c) are the plots of DOS for CoFe alloys respectively. And the values of spin-splitting (SS) have been calculated thoroughly. Among all the compositions of Co_xFe_{1x}, $Co_{25}Fe_{75}$ alloy shows the highest value of SS because of the higher content of Fe as it already has the largest value of SS, as mentioned in table 7).

(II) $Ni_x Fe_{1-x}$ Alloys

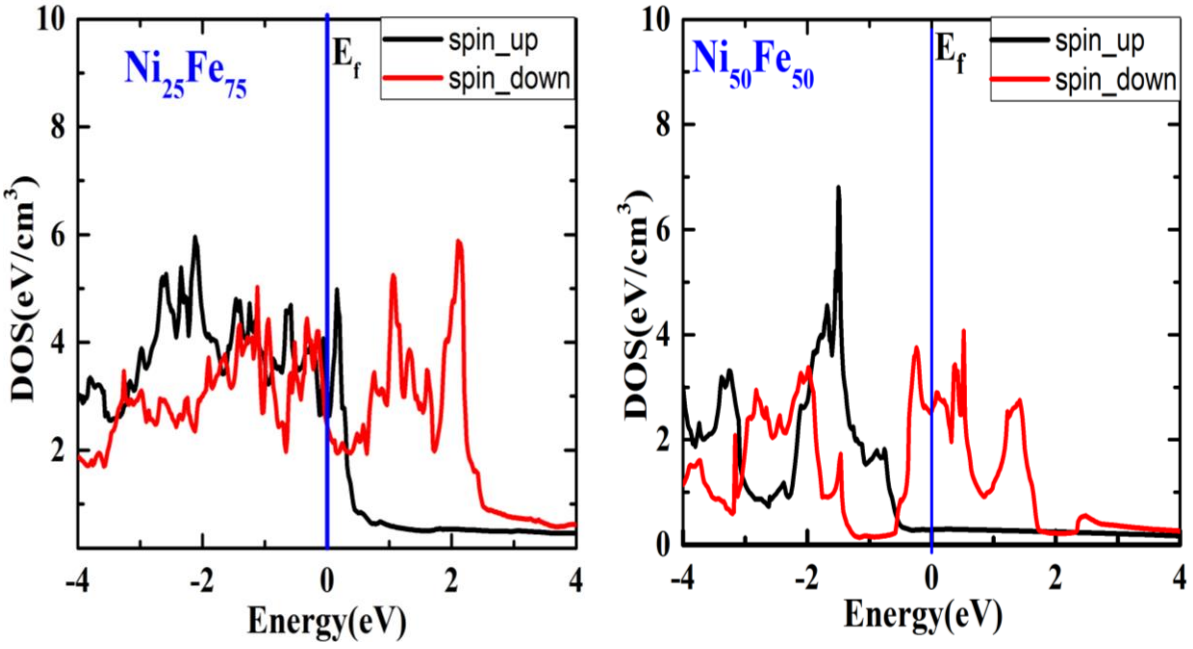

(a) **(b)**

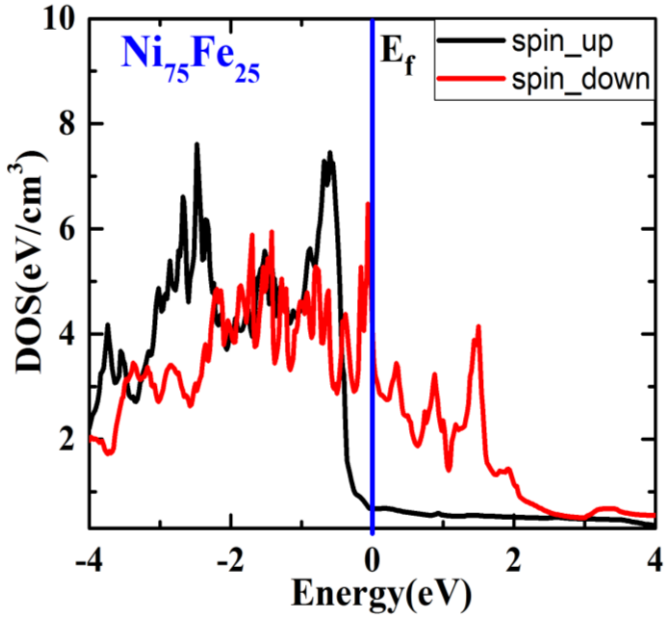

(c)

Figure 14. DOS for different configurations of Ni_xFe_{1-x} alloys.

In **Figure 14**, (a),(b) and (c) represents the plots of DOS for NiFe alloys respectively and then spin-splitting (SS) values have been calculated thoroughly. Among all the compositions of Ni_xFe_{1-x}, $Ni_{25}Fe_{75}$ alloy shows the largest value of SS.

(III) $Co_x Ni_{1-x}$ Alloys

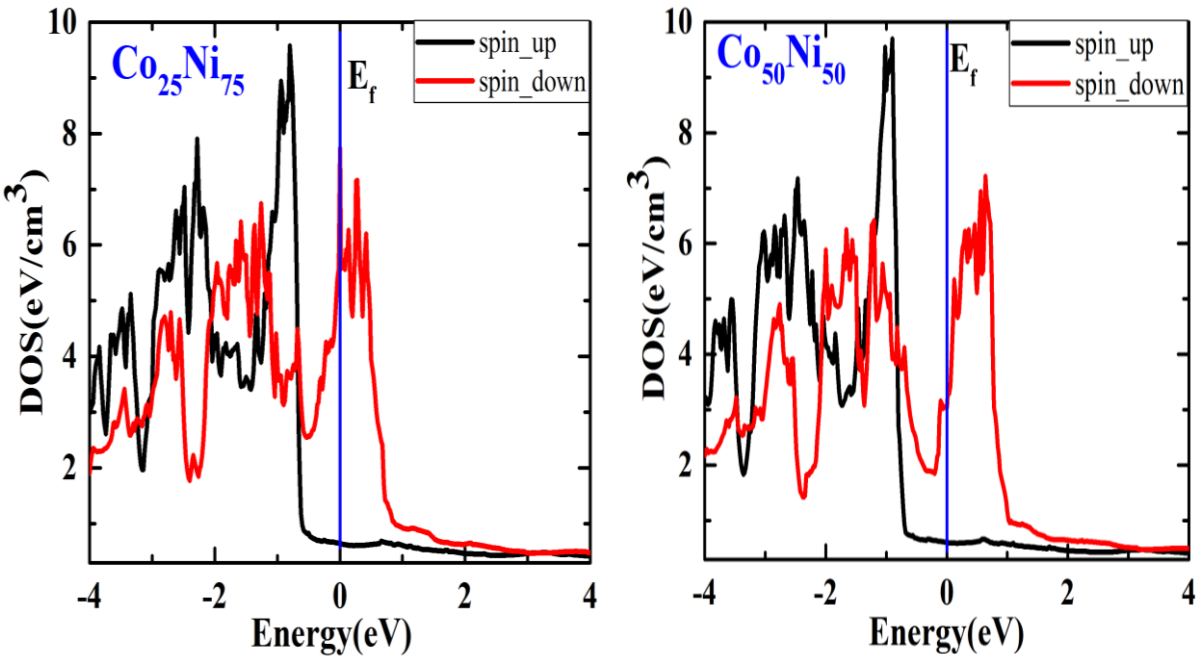

(a) **(b)**

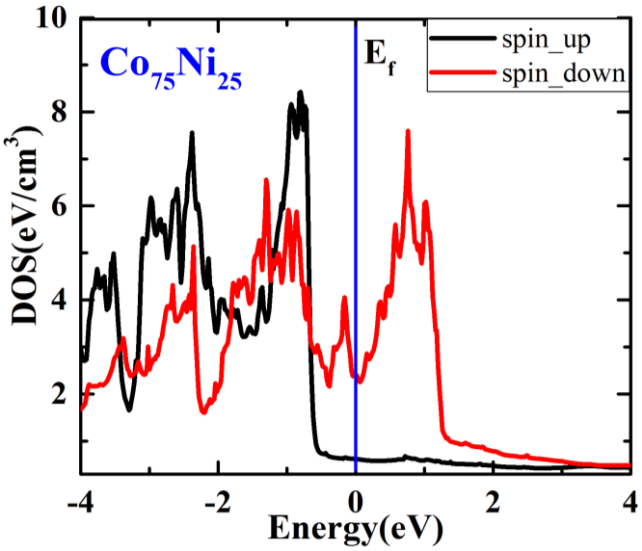

(c)

Figure 15. DOS for different configurations of Co_xNi_{1-x} alloys.

In **Figure 15**, (a), (b) and (c) represents the plots of DOS for NiFe alloys respectively and then values of spin-splitting (SS) have been calculated thoroughly. Among all the compositions of Co_xNi_{1-x}, $Co_{25}Ni_{75}$ alloy shows the largest value of SS.

After the plots of DOS, we have calculated the values of spin-splittings for all the ferromagnetic alloys which are used in our work and a table of these values is given as below;

Ferromagnetic alloys	**SS (eV)**
$Co_{25}Fe_{75}$	2.20
$Co_{50}Fe_{50}$	2.16
$Co_{75}Fe_{25}$	2.12
$Ni_{25}Fe_{75}$	1.80
$Ni_{50}Fe_{50}$	1.90
$Ni_{75}Fe_{25}$	1.98
$Co_{25}Ni_{75}$	1.90
$Co_{50}Ni_{50}$	1.75
$Co_{75}Ni_{25}$	1.50

Table 8. Values of spin-splitting for various permalloys.

4.3 Parameters and Simulation

Based on obtained results from electronic structure properties such as band structures, DOS and spin-splitting, the possibility of using these materials in the proposed device is concluded. QuantumATK (atomistix toolkit) is used to study the properties of these materials at the atomistic level and is also used to obtain the material parameters for simulation purpose. After collecting other data like M_s, $H_{k,}$ α, and U_b for all possible materials and their alloys by following the given tables, simulation has been performed in 'NanoHub' software, where we observe how the variation in parameters of an MTJ is taking place concerning the applied voltage. These parameters of MTJ are resistance, TMR, and STT components. And all these parameters are plotted as below sections;

4.3.1 Simulation for the ferromagnetic materials

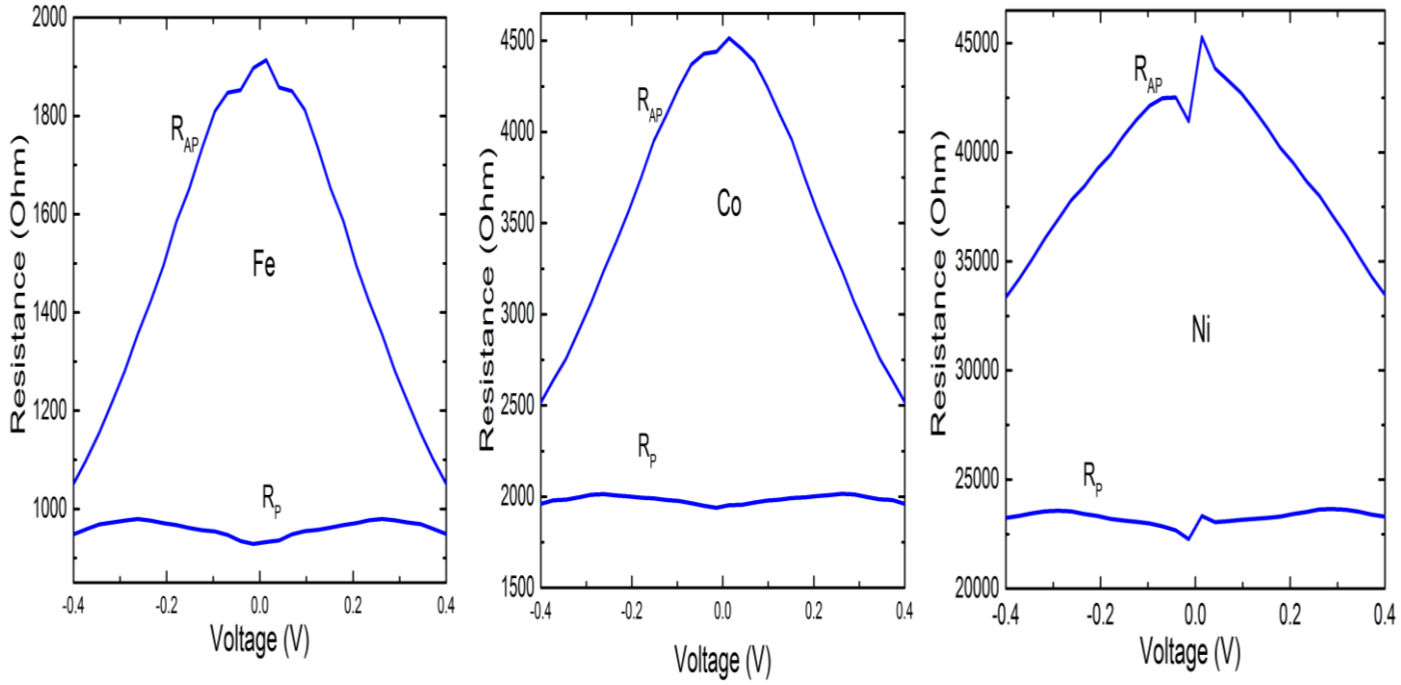

Figure 16. Resistance vs Voltage plot for the different FM.

The above **Figure 16** shows the variation of both the resistances (R_P and R_{AP}) wrt the voltage supply. Here, Ni exhibits a sharp discontinuity and non-symmetry over the supply because of the less splitting of spins (experimentally found). In contrast, Fe has been seen as having more symmetry and continuity, and Co shows in-between characteristics.

After the plots of resistances, we move for the TMR plot by following equation (I). The values of TMR are obtained following R_P and R_{AP} values for different FM and these plots have been shown in **Figure 17**.

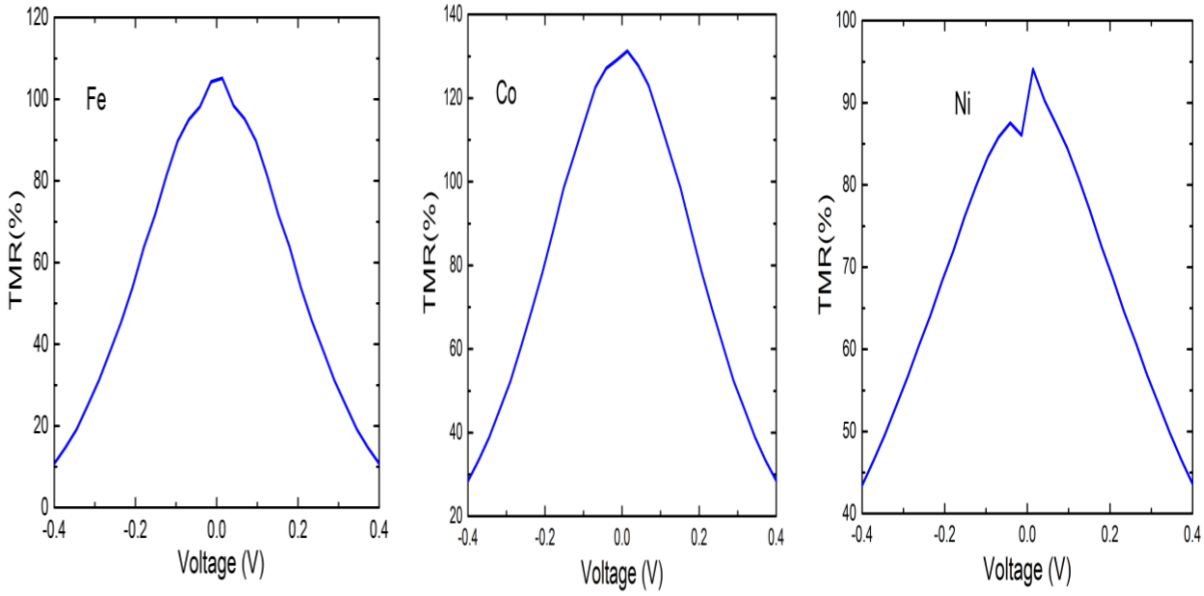

Figure 17. Plots for TMR vs Voltage supply for all FM.

For an MTJ device, TMR is an important and well-known attribute and **Figure 17** represents the plot of TMR for the different FM. All these graphs clearly show that the Co-based device (see **Figure 17b**) has better TMR than the Fe and Ni-based device (**Figure 17a and 17c**). It has followed according to the relative difference between R_P and R_{AP} values as mentioned in **Figure 16**. Basically, TMR is used for 'READ' bit by determining whether the electrodes have magnetic moments in the parallel or antiparallel state. Hence, as the higher TMR, the capability of bits resolving for that particular device will be better. Therefore, according to our observation Co-based MTJ device has a better stable memory state.

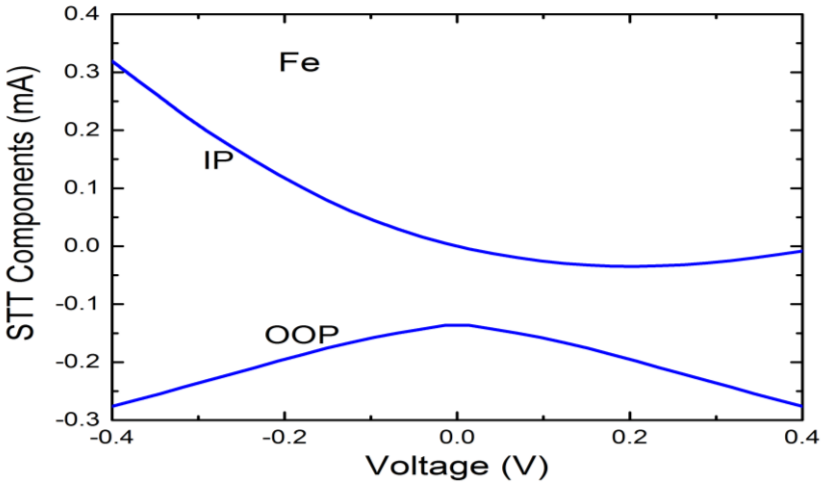
Fe
IP
OOP
STT Components (mA)
Voltage (V)
0.4
0.3
0.2
0.1
0.0
-0.1
-0.2
-0.3
-0.4
-0.2
0.0
0.2
0.4

(a)

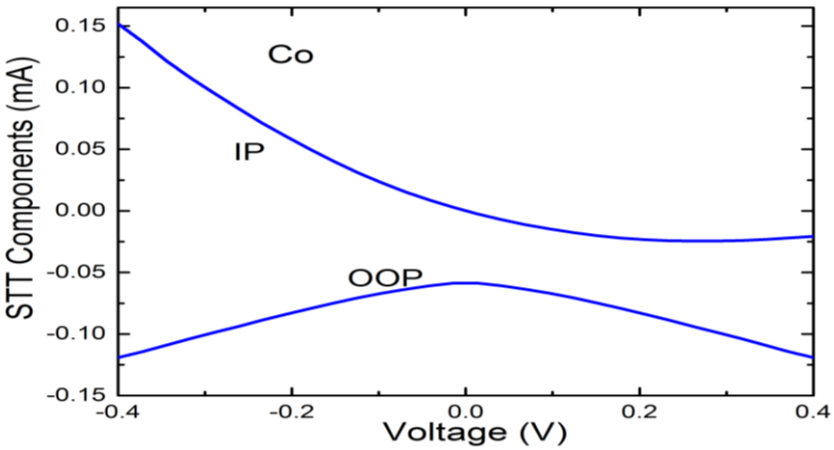
Co
IP
OOP
STT Components (mA)
Voltage (V)
0.15
0.10
0.05
0.00
-0.05
-0.10
-0.15
-0.4
-0.2
0.0
0.2
0.4

(b)

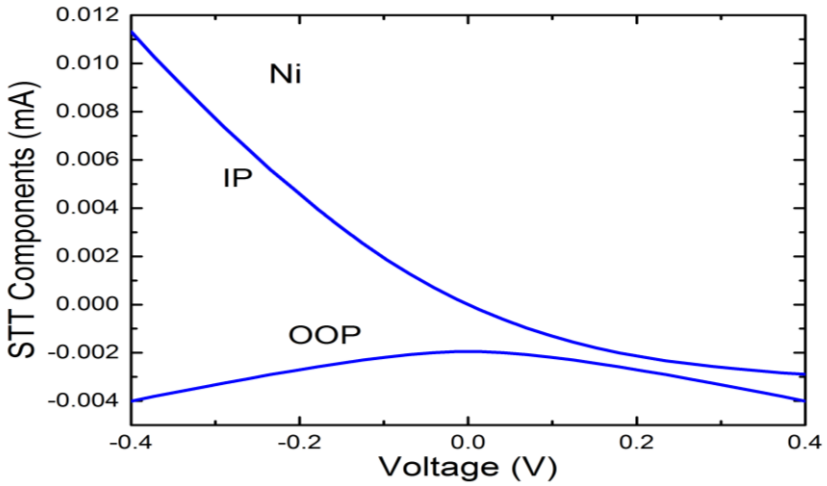
Ni
IP
OOP
STT Components (mA)
Voltage (V)
0.012
0.010
0.008
0.006
0.004
0.002
0.000
-0.002
-0.004
-0.4
-0.2
0.0
0.2
0.4

(c)

Figure 18. Plots for the STT components of different FM.

Figure 18 shows STT components in both planes (IP and OOP) with respect to supply voltage. It has been observed from those plots that the STT current performance of the Fe-based device is excellent. However, the STT current components of the Co and Ni-based device are also good, but the performance in these two devices is far below as compared to the Fe- based MTJ device. The conduction electrons of non-equilibrium state exert an equal, but opposite torque to the re-oriented spins in the FM establish the STT components. The strength of spin orientation and probability of spin transfer taking place from the reference layer to the free layer in an MTJ is governed by the net change in spin-current before and after the interaction of the electron spin and magnetic moment. Therefore, better performance of STT component exhibits more robust and better spin-alignment.

4.3.2 Simulation for ferromagnetic alloys

(I)Co_xFe_{1-x}

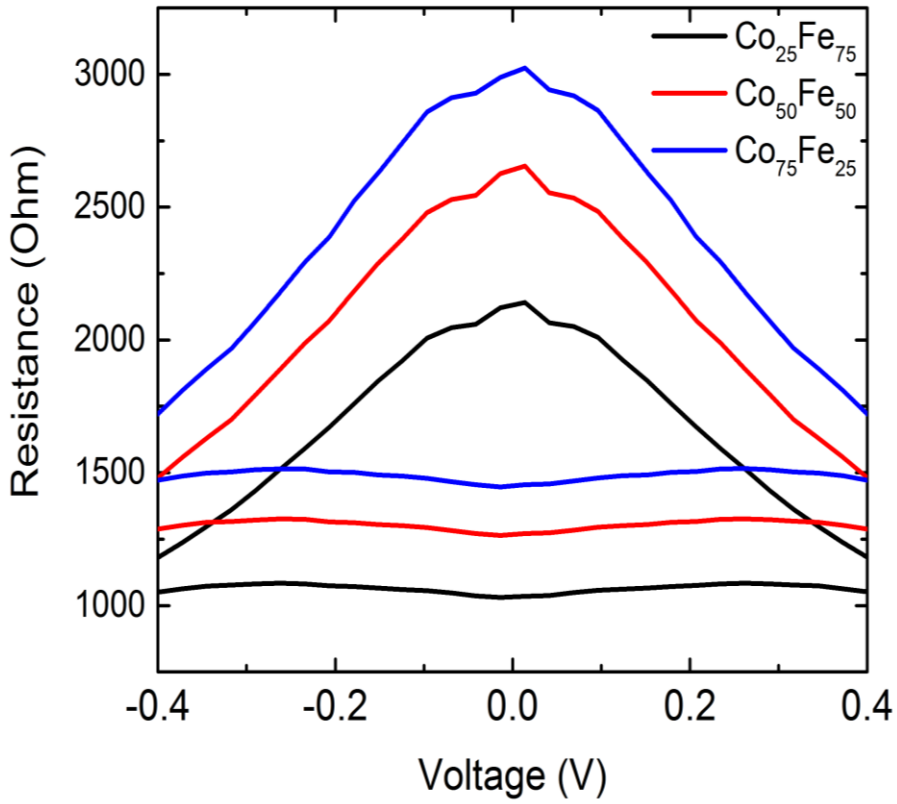

Figure 19. Resistance plots for the different configurations of Co_xFe_{1-x} alloys.

Figure 19 shows the variation of resistances in antiparallel (R_{AP})and parallel (R_P) states with various configurations of Co_xFe_{1-x} alloys. As the composition of Co increases in Fe, resistances also increase and based on these variations; the TMR values are calculated and plotted accordingly in **Figure 20**. One should have to consider all the parameters and factors causing variations in resistances as well as in TMRs.

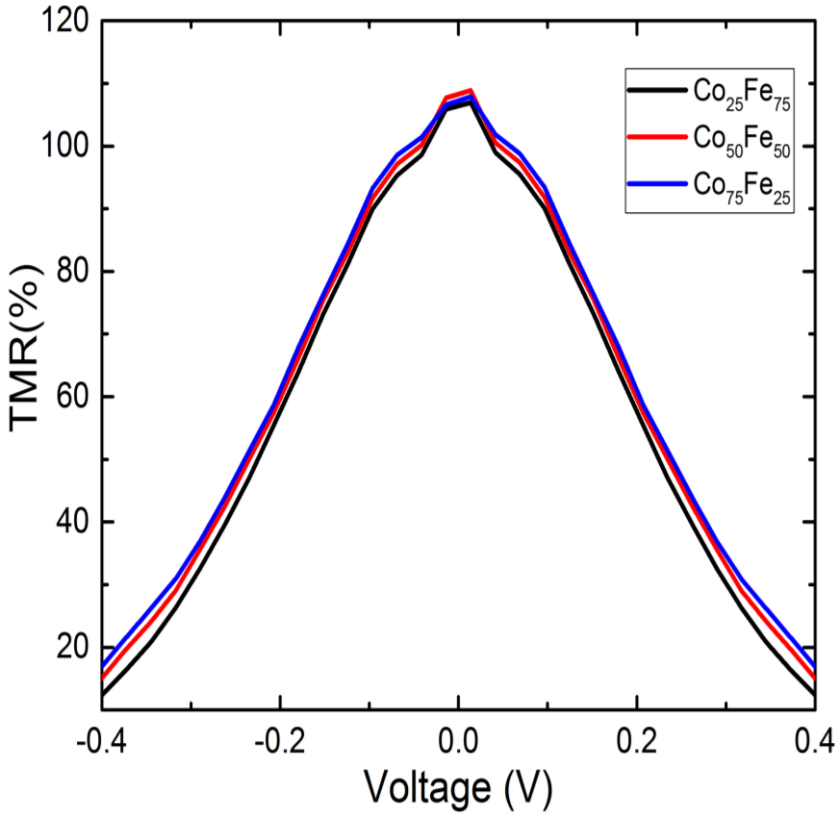

Figure 20. TMR plots for different configurations of Co_xFe_{1-x} alloys.

According to the above plot, it can be observed that $Co_{50}Fe_{50}$ shows maximum TMR value throughout all the configurations (**Figure 20**). So it can be used as a better candidate in the case of CoFe alloys. **Figure 21** is about the variations of STT components of CoFe alloys and these decrease with Co's increasing composition in Co_xFe_{1-x} alloy. $Co_{25}Fe_{75}$ shows the maximum value for STT components.

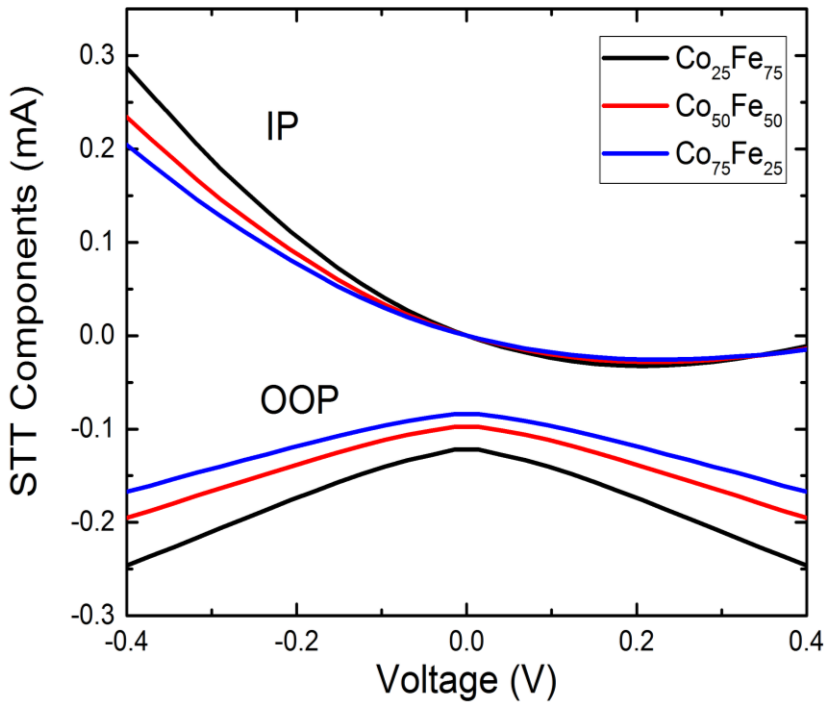

Figure 21. STT components plot for different configurations of Co_xFe_{1-x} alloys.

(II)Ni_xFe_{1-x}

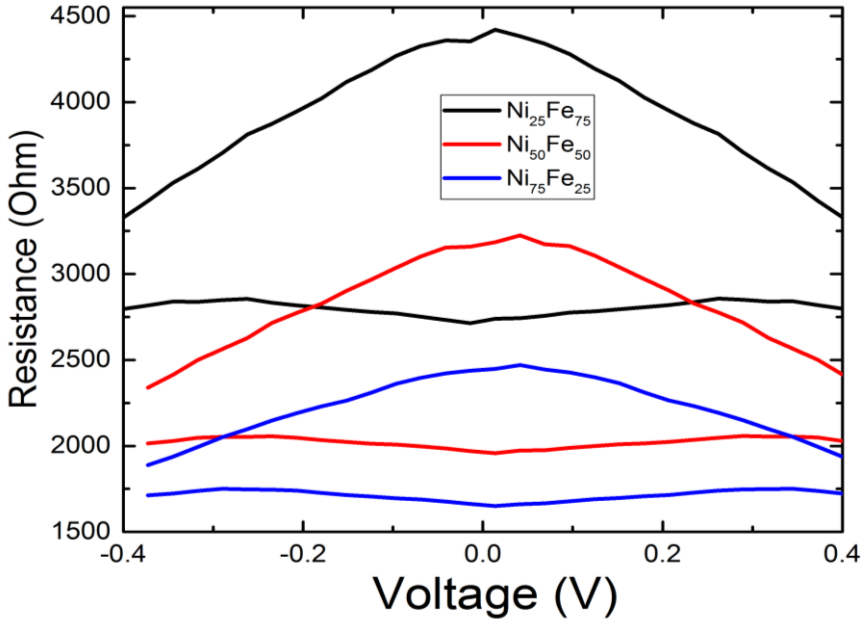

Figure 22. Resistance plots for different configurations of Ni_xFe_{1-x} alloys.

Figure 22 shows the variation of resistances in antiparallel (R_{AP})and parallel (R_P) state with various configurations of Ni_xFe_{1-x} alloys. As the composition of Ni increases in Fe, resistances decreased and based on these variations; the TMR values are calculated and plotted accordingly in figure 23. TMR value increases as the Ni-content decreases, but due to the fact of others parameters, we have found the maximum value of TMR for the $Ni_{50}Fe_{50}$ among all the configurations of Ni_xFe_{1-x} .

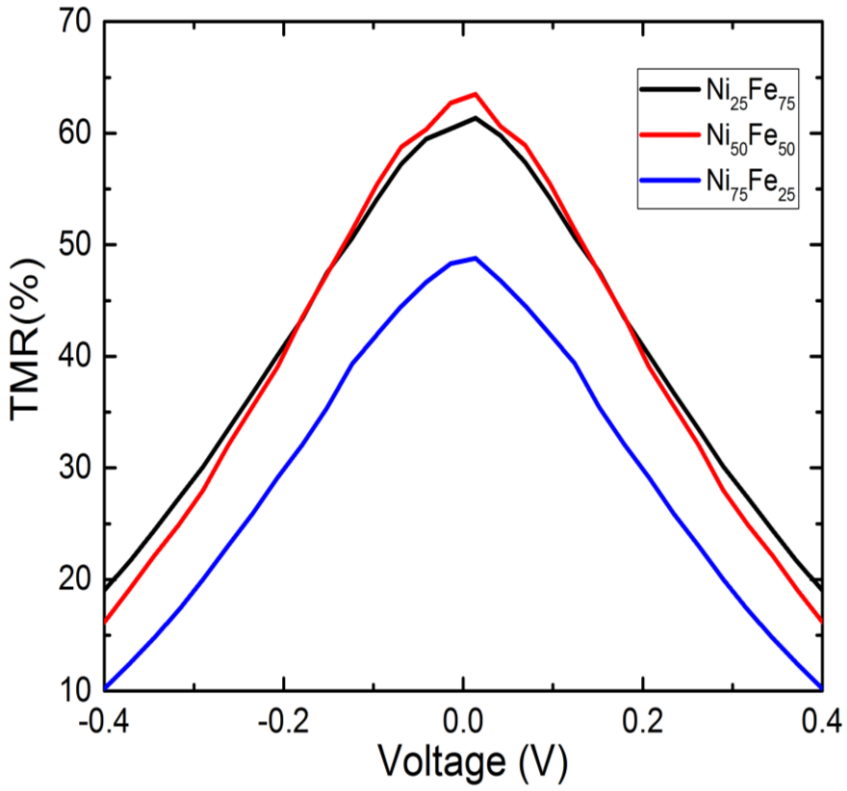

Figure 23. TMR plots for different configurations of Ni_xFe_{1-x} alloys.

Figure 23 shows the variation of STT components of Ni_xFe_{1-x} alloys and these increase with the increasing composition of Ni in Fe and $Ni_{75}Fe_{25}$ shows the maximum value for STT components among all the configurations of Ni_xFe_{1-x} .

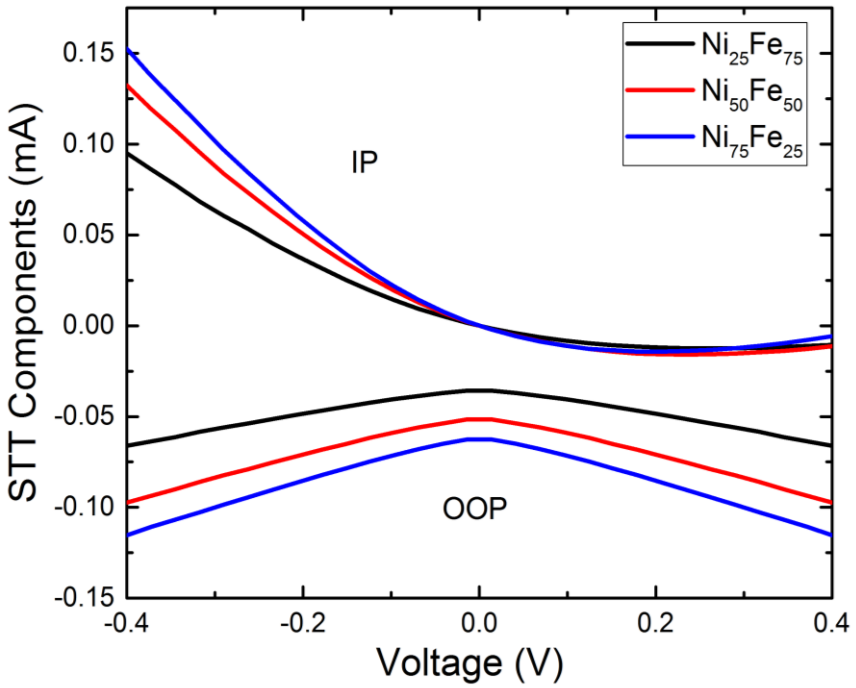

Figure 24. STT component plots of various compositions of Ni_xFe_{1-x} alloys.

(III) Co_xNi_{1-x}

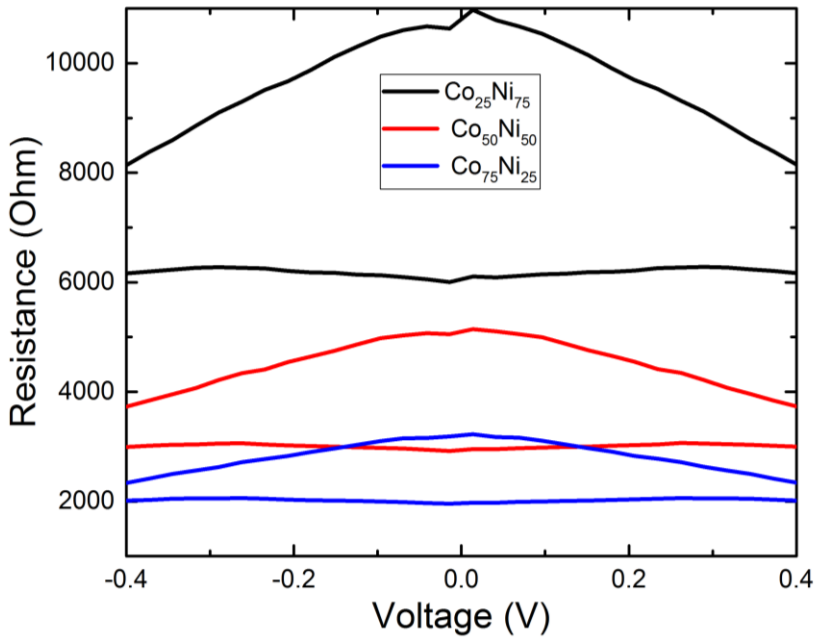

Figure 25. Resistance plots for different configurations of Co_xNi_{1-x} alloys.

Figure 25 shows the variation of resistances in antiparallel (R_{AP})and parallel (R_P) state with various configurations of Co_xNi_{1-x} alloys. As the composition of Co increases in Ni, resistances decreased and based on these variations, the TMR values are calculated and plotted accordingly in **Figure 26**. TMR value decreases with the Co-content, but due to others parameters, we have found the maximum value of TMR for the $Co_{25}Ni_{75}$ among all the configurations of Co_xNi_{1-x}.

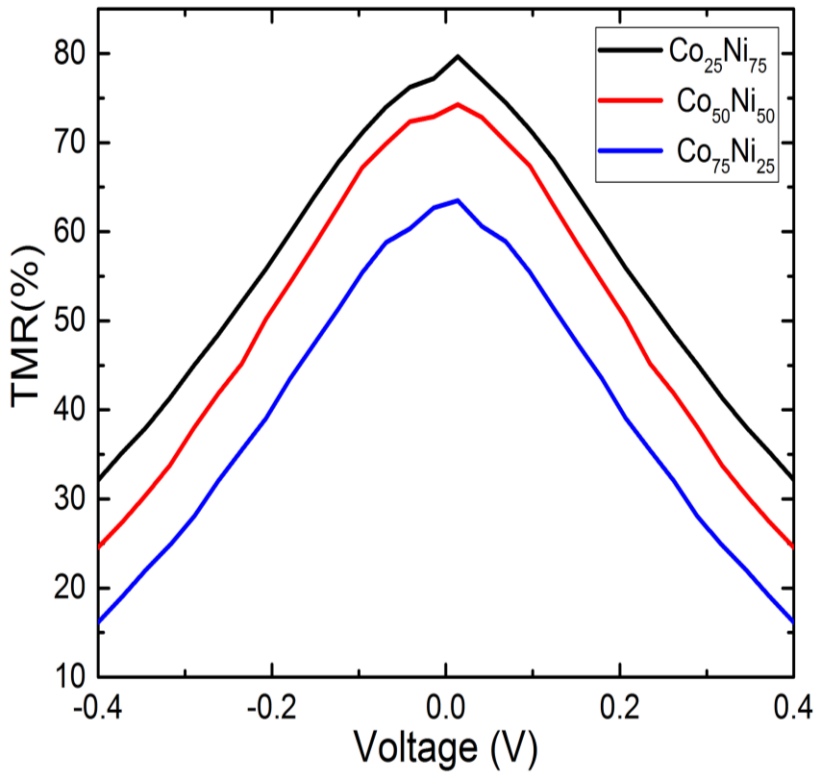

Figure 26. TMR plots for different configurations of Co_xNi_{1-x} alloys.

Figure 27 shows a plot for the variation of STT components of Co_xNi_{1-x} alloys and these increase with the increasing composition of Co in Ni and $Co_{75}Ni_{25}$ offers the maximum value for STT components among all the configurations of Co_xNi_{1-x}.

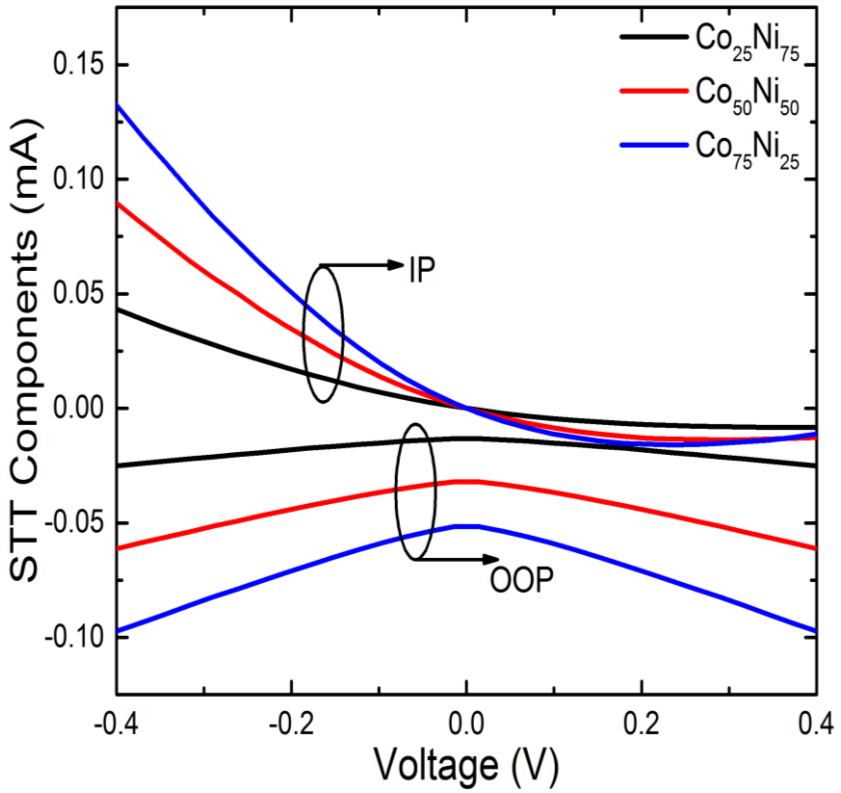

Figure 27. STT components plots of various compositions of Co_xNi_{1-x} alloys.

CHAPTER5

COMPARISON AND CONCLUSION

We calculated tunnelling magnetoresistance (TMR) in an MTJ of FM/MgO/FM using the NEGF technique as implemented in the nanoHUB simulation tool. We compared the TMRs of the CoFe-based, NiFe-based and CoNi-based electrodes, and it was found out that the CoFe-based electrodes c produce a much higher TMR. And the composition $Co_{50}Fe_{50}$ shows the maximum TMR value for the MTJ. The bandstructure of the electrodes was calculated using DFT first-principles calculation. The results are in range with the experimentally reported data. However, making contact between metal and insulator would induce a few states within the energy gap of the interfacial layers at the interface, known as the metal-induced gap states, and that we have not taken into consideration for our calculations.

References

[1] K. Y. Camsari, S. Ganguly, and S. Datta, “Modular approach to spintronics,” *Sci. Rep.*, vol. 5, no. May, 2015, doi: 10.1038/srep10571.

[2] M. A. W. Schoen, “Magnetic damping in binary 3-d transition metal alloys and multilayers,” *PhD Thesis*, 2017, [Online]. Available: https://epub.uni-regensburg.de/35780/1/dr_arbeit-FINAL - Published version.pdf.

[3] S. Bhatti, R. Sbiaa, A. Hirohata, H. Ohno, S. Fukami, and S. N. Piramanayagam, “Spintronics based random access memory: a review,” *Mater. Today*, vol. 20, no. 9, pp. 530–548, 2017, doi: 10.1016/j.mattod.2017.07.007.

[4] J. H. Oh *et al.*, “A novel process for highly manufacturable MRAM,” *J. Magn. Magn. Mater.*, vol. 272–276, no. III, pp. 1936–1938, 2004, doi: 10.1016/j.jmmm.2003.12.1190.

[5] M. Properties, “Magnetic Properties • 803 (,” no. c, pp. 803–837.

[6] A. M. Joshi and S. Balecha, “Magnetic Tunnel Junction Based Applications and Logic Computation,” vol. 3, no. 1, pp. 15–21, 2016.

[7] T. F. Device, *Agglications Thin Film Device A { lfllications AND. .*

[8] D. Apalkov, B. Dieny, and J. M. Slaughter, “Magnetoresistive Random Access Memory,” vol. 104, no. 10, 2016.

[9] И. В. Павлова, М. П. Рысакова, and М. И. Сергеева, “Влияние Блокады D1 И D2 Рецепторов В Базолатеральной Миндалине На Поведение Крыс С Высоким И Низким Уровнем Тревожности И Страха,” *Журнал Высшей Нервной Деятельности Им. И. В. Павлова*, vol. 65, no. 4, pp. 471–485, 2015, doi: 10.7868/s0044467715030065.

[10] J. Mathon and A. Umerski, “J. Mathon and A. Umerski,” vol. 63, pp. 1–4, 2001, doi: 10.1103/PhysRevB.63.220403.

[11] D. C. Ralph and M. D. Stiles, “Spin transfer torques,” *J. Magn. Magn. Mater.*, vol. 320, no. 7, pp. 1190–1216, 2008, doi: 10.1016/j.jmmm.2007.12.019.

[12] S. Ikeda *et al.*, “Magnetic tunnel junctions for spintronic memories and beyond,” *IEEE Trans. Electron Devices*, vol. 54, no. 5, pp. 991–1002, 2007, doi: 10.1109/TED.2007.894617.

[13] S. Z. Peng, Y. Zhang, M. X. Wang, Y. G. Zhang, and W. Zhao, “Magnetic Tunnel Junctions for Spintronics: Principles and Applications,” *Wiley Encycl. Electr. Electron. Eng.*, vol. 1936, no. 12, pp. 1–16, 2014, doi: 10.1002/047134608x.w8231.

[14] C. Park, “Magnetic tunnel Fueled by the ever-increasing demand for larger hard disk drive storage,” vol. 9, no. 11, pp. 36–45, 2006, doi: 10.1016/S1369-7021(06)71693-5.

[15] C. Heiliger, P. Zahn, and I. Mertig, “Microscopic origin of magnetoresistance Tunneling magnetoresistance is one of the basic effects of spintronics are discussed for one of the standard systems , Fe / MgO / Fe .,” vol. 9, no. 11, pp. 46–54, 2006, doi: 10.1016/S1369-7021(06)71694-7.

[16] S. Ganguly, “Magnetic Tunnel Junction Lab v1 . 0 : User Manual,” pp. 1–12, 2014.

[17] Y. Zhang, X. Wang, Y. Li, A. K. Jones, and Y. Chen, “Asymmetry of MTJ switching and its implication to STT-RAM designs,” in *2012 Design, Automation & Test in Europe Conference & Exhibition (DATE)*, 2012, pp. 1313–1318.

[18] N. Umetsu, D. Miura, and A. Sakuma, “Microscopic theory on the Gilbert damping due to spin pumping effects in the magnetic multi-layer system,” *J. Phys. Conf. Ser.*, vol. 266, no. 1, 2011, doi: 10.1088/1742-6596/266/1/012084.

[19] M. Mohanta *et al.*, “Structural and magnetic properties of CoNi surface alloys,” *Phys. B Condens. Matter*, vol. 572, no. September, pp. 105–108, 2019, doi: 10.1016/j.physb.2019.07.032.

[20] S. Azzawi, A. T. Hindmarch, and D. Atkinson, “Magnetic damping phenomena in ferromagnetic thin-films and multilayers,” *J. Phys. D. Appl. Phys.*, vol. 50, no. 47, 2017, doi: 10.1088/1361-6463/aa8dad.

[21] Y. R. Jang and B. D. Yu, “Electronic structures and spin magnetic properties of CoFe: Lattice strain effects,” *J. Korean Phys. Soc.*, vol. 60, no. 3, pp. 445–449, 2012, doi: 10.3938/jkps.60.445.

[22] M. Bedir, Ö. F. Bakkaloğlu, I. H. Karahan, and M. Öztaş, “A study on electrodeposited NixFe1-x alloy films,” *Pramana - J. Phys.*, vol. 66, no. 6, pp. 1093–1104, 2006, doi:

10.1007/BF02708462.

[23] A. Melloul and A. Kharmouche, “Synthesis, structure and magnetic properties of CoxFe100–x thin films thermally evaporated onto Si (111) substrate,” *J. Mater. Sci. Mater. Electron.*, vol. 30, no. 14, pp. 13144–13150, 2019, doi: 10.1007/s10854-019-01677-3.

[24] “IEEE Transactions on Magnetics,” *IEEE Trans. Magn.*, vol. 24, no. 6, pp. 2300–3179, 1988, doi: 10.1109/20.92092.

[25] G. S. D. Beach and A. E. Berkowitz, “Co-Fe metal/native-oxide multilayers: A new direction in soft magnetic thin film design I. quasi-static properties and dynamic response,” *IEEE Trans. Magn.*, vol. 41, no. 6, pp. 2043–2052, 2005, doi: 10.1109/TMAG.2005.847631.

[26] X. Su and C. Qiang, “Influence of pH and bath composition on properties of Ni – Fe alloy films synthesized by electrodeposition,” vol. 35, no. 2, pp. 183–189, 2012.

[27] W. J. Fan, L. Ma, Z. Shi, and S. M. Zhou, “Fabrication and magnetocrystalline anisotropy of NiCo(002) films,” *Chinese Phys. B*, vol. 24, no. 3, pp. 2–6, 2015, doi: 10.1088/1674-1056/24/3/037507.

[28] B. A. Mazin, “Thesis by,” vol. 2004, 2004.

[29] W. H. Butler, X. G. Zhang, T. C. Schulthess, and J. M. MacLaren, “Spin-dependent tunneling conductance of Fe/MgO/Fe sandwiches,” *Phys. Rev. B - Condens. Matter Mater. Phys.*, vol. 63, no. 5, pp. 544161–5441612, 2001, doi: 10.1103/physrevb.63.054416.

[30] F. Bonell *et al.*, “Spin-polarized electron tunneling in bcc FeCo/MgO/FeCo(001) magnetic tunnel junctions,” *Phys. Rev. Lett.*, vol. 108, no. 17, 2012, doi: 10.1103/PhysRevLett.108.176602.

[31] S. Yuasa and D. D. Djayaprawira, “Giant tunnel magnetoresistance in magnetic tunnel junctions with a crystalline MgO(0 0 1) barrier,” *J. Phys. D. Appl. Phys.*, vol. 40, no. 21, 2007, doi: 10.1088/0022-3727/40/21/R01.

[32] B. A. Ali and N. K. Allam, “A first-principles roadmap and limits to design efficient supercapacitor electrode materials,” *Phys. Chem. Chem. Phys.*, vol. 21, no. 32, pp. 17494–17511, 2019, doi: 10.1039/c9cp02614b.

[33] W. Kohn, A. D. Becke, and R. G. Parr, "Density functional theory of electronic structure," *J. Phys. Chem.*, vol. 100, no. 31, pp. 12974–12980, 1996, doi: 10.1021/jp960669l.

[34] M. Noe, R. Heller, W. H. Fietz, W. Goldacker, and T. Schneider, "HTS applications," *Proc. - Work. Accel. Magn. Supercond. Des. Optim. WAMSDO 2008*, pp. 94–97, 2009.

[35] W. Lafayette, "Nanoscale device modeling : the Green ' s function method," vol. 28, no. 4, 2000, doi: 10.1006/spmi.2000.0920.

[36] Z. Qian, R. Li, S. Hou, Z. Xue, and S. Sanvito, "An efficient nonequilibrium Green's function formalism combined with density functional theory approach for calculating electron transport properties of molecular devices with quasi-one-dimensional electrodes," *J. Chem. Phys.*, vol. 127, no. 19, 2007, doi: 10.1063/1.2804876.

[37] M. P. Anantram, M. S. Lundstrom, and D. E. Nikonov, "Modeling of nanoscale devices," *Proc. IEEE*, vol. 96, no. 9, pp. 1511–1550, 2008, doi: 10.1109/JPROC.2008.927355.

[38] M. J. S. V. M. C, "Nonequilibrium Green ' s function approach to the magnetotransport in magnetic tunnel junctions exhibiting quasiparticle bands," vol. 41, no. 2009, p. 2010.

[39] M. Paulsson, "Non Equilibrium Green's Functions for Dummies: Introduction to the One Particle NEGF equations," pp. 1–9, 2002, [Online]. Available: http://arxiv.org/abs/cond-mat/0210519.

[40] B. Sharma, A. Mukhopadhyay, L. Banerjee, A. Sengupta, H. Rahaman, and C. K. Sarkar, "Ab initio study of mono-layer 2-D insulators (X-(OH)2 and h-BN) and their use in MTJ memory device," *Microsyst. Technol.*, vol. 25, no. 5, pp. 1909–1917, 2019, doi: 10.1007/s00542-018-3728-2.